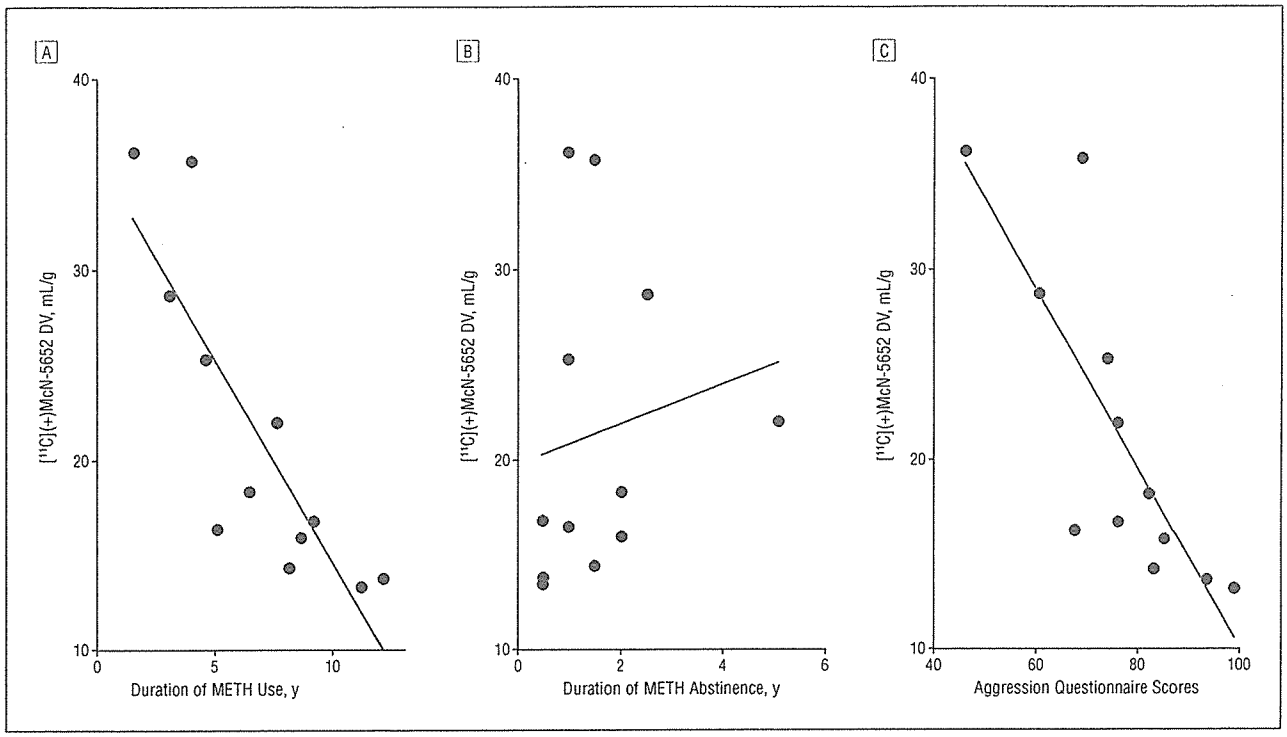

Figure 3. Correlations between *trans*-1,2,3,5,6,10-beta-hexahydro-6-[4-(methylthio)phenyl]pyrrolo-[2,1-a]isoquinoline ([^{11}C](+)McN-5652) distribution volumes (DVs) in a representative brain region (the thalamus) and clinical variables in methamphetamine (METH) abusers. A, Significant negative correlation between [^{11}C](+)McN-5652 DVs and the duration of METH use (r=−0.84; P=.001 by Pearson correlation coefficient). B, Correlation between [^{11}C](+)McN-5652 DVs and the duration of METH abstinence (r=0.16; P=.61). C, Correlation between Aggression Questionnaire scores and [^{11}C](+)McN-5652 DVs (r=−0.82; P=.001).

Although the present study was not designed to directly assess recovery from brain damage induced by methamphetamine use, there was no correlation between the [^{11}C](+)McN-5652 DVs and the duration of methamphetamine abstinence. Along with this finding, the result showing that even individuals who had been abstinent for more than 1 year (n=9) had a substantial decrease in serotonin transporter density (approximately a 30% decrease compared with controls) (Figure 3B) suggests that reductions in the density of the serotonin transporter in the brain associated with habitual methamphetamine abuse could persist long after methamphetamine use ceases.

The magnitude of aggression in methamphetamine abusers increased significantly with decreasing serotonin transporter densities in some brain regions. Detoxification from methamphetamine in all the abusers in this study was confirmed by regular urine drug screening as described in the "Drug Screening" subsection, including a test on the day of PET examination; these tests were conducted to establish that the psychiatric symptoms, such as aggression, were residual rather than acute symptoms induced by methamphetamine use. As a result, the relationship between the degree of aggressiveness and the density of serotonin transporter found in this study was not ascribed to the process of detoxification from methamphetamine use. Thus, the present findings indicate that methamphetamine-induced serotonergic disturbances are responsible for the elevated aggressiveness that is frequently observed, as a residual symptom, in abstinent methamphetamine abusers. This contention is consistent with a variety of studies[52,53] that have documented associations between decreased serotonergic function and increased aggression. For example, cerebrospinal fluid 5-hydroxyindoleacetic acid, which is known to reflect presynaptic serotonergic activity in the brain, has been found to be reduced in aggressive psychiatric patients,[54,55] impulsive violent men,[56,57] and impulsive violent offenders.[58]

In the correlational region analysis using SPM in the methamphetamine group, the magnitude of aggression was substantially associated with a decrease in serotonin transporter density in the clusters located in the orbitofrontal cortex, anterior cingulate, and temporal cortex, although the clusters were localized to small areas and did not fully occupy the anatomic brain regions. This result suggests that the potential methamphetamine-induced decrease in serotonergic function around these 3 areas may play an important role in the pathogenesis of elevated aggression in methamphetamine abusers. This is supported by several lines of evidence. For example, studies of brain injuries suggest that damage to the orbitofrontal and anterior cingulate areas produces syndromes characterized by aggression and impulsivity.[52,59] Furthermore, recent PET and postmortem clinicopathologic correlation studies have indicated that low levels of serotonin$_{1A}$ receptors in the orbitofrontal, anterior cingulate gyrus, and temporal areas are related to aggressive behavior.[60,61]

However, we cannot rule out the possibility that the increased aggression observed in methamphetamine abusers could reflect a preexisting condition, for example, an "addictive personality," which might often involve a tendency toward aggression.[62] Nevertheless, in the present study, we selected methamphetamine abusers who had no history of abnormal aggression before the use of meth-

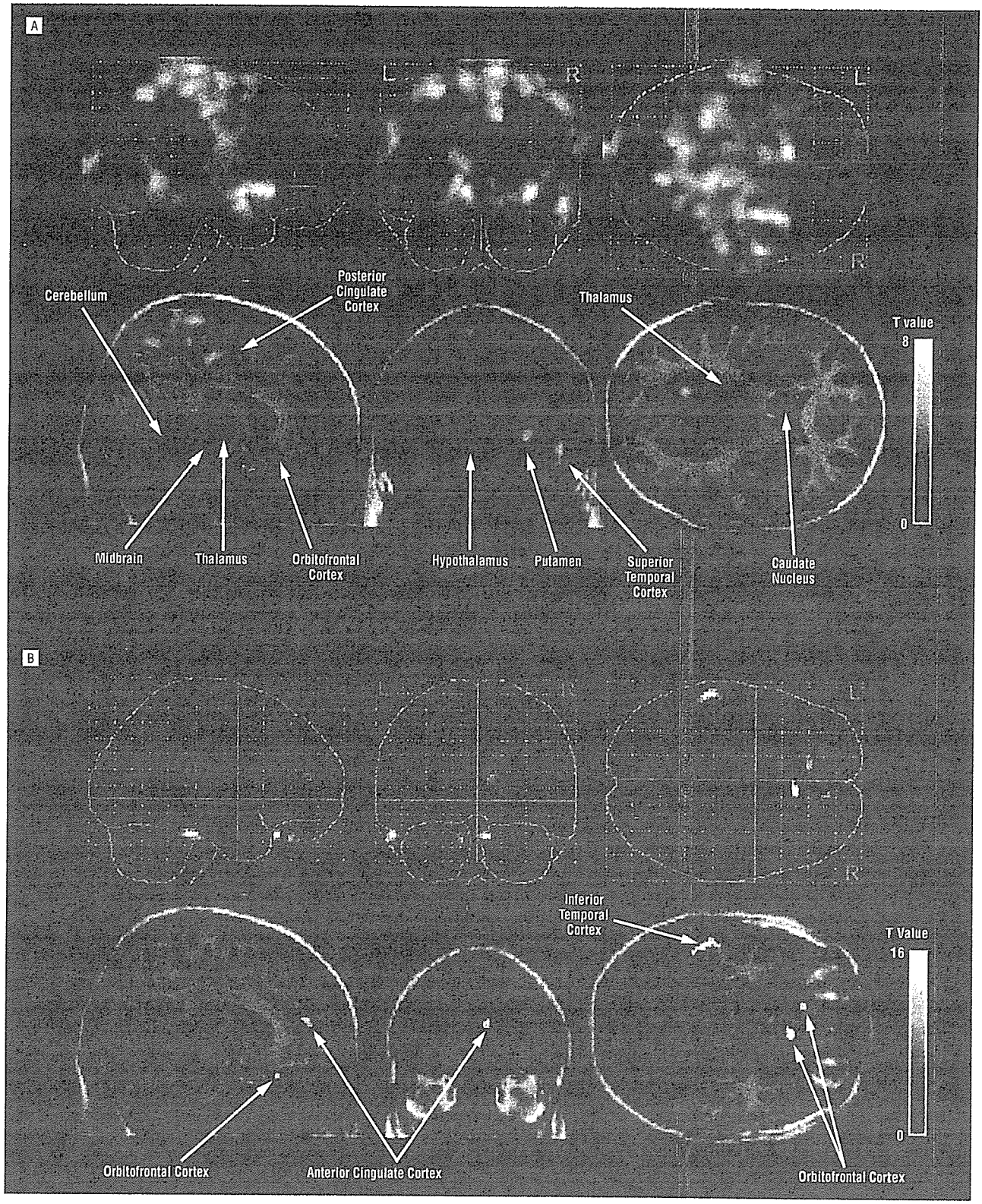

Figure 4. Results of the whole-brain voxel-based statistical parametric mapping analysis of the *trans*-1,2,3,5,6,10-beta-hexahydro-6-[4-(methylthio) phenyl]pyrrolo-[2,1-a]isoquinoline ([^{11}C](+)McN-5652) distribution volumes (DVs). A, Locations of methamphetamine abuser and control differences in [^{11}C](+)McN-5652 DVs. Areas with significantly reduced [^{11}C](+)McN-5652 DVs in methamphetamine abusers compared with those in controls ($P<.001$, corrected for cluster level) are given in Table 2. B, Locations of clusters with significant negative correlations between Aggression Questionnaire scores and [^{11}C](+)McN-5652 DVs in methamphetamine abusers ($P<.05$, corrected for voxel level) (Table 3). Each top row shows 3-dimensional glass brain views; each bottom row, detected area superimposed onto normal template magnetic resonance images.

amphetamine, and their histories were retrospectively confirmed by the abusers and their family members through detailed Structured Clinical Interview for *Diagnostic and Statistical Manual of Mental Disorders, Fourth Edition–*

Table 2. Voxel-Based Analysis of Regional Brain [^{11}C](+)McN-5652 Distribution Volume Reductions in 12 Methamphetamine Abusers Compared With 12 Control Subjects*

	Cluster-Level Analysis		Voxel-Level Analysis		Talairach Coordinates		
Location	Corrected *P* Value	Voxels, No.	Corrected *P* Value	*z* Score	x	y	z
Right insular cortex	<.001	45315	.009	5.33	34	13	−4
Left caudate nucleus	NA	NA	.02	5.12	−10	19	−4
Right claustrum	NA	NA	.03	5.02	32	0	−3

Abbreviations: [^{11}C](+)McN-5652, *trans*-1,2,3,5,6,10-beta-hexahydro-6-[4-(methylthio)phenyl]pyrrolo-[2,1-a]isoquinoline; NA, not available.
*The significance threshold was $P<.05$ at the corrected voxel level and $P<.05$ at the corrected cluster level. Coordinates are given in millimeters from the origin at the midpoint of the anterior commissure for voxels of peak significance.

Table 3. Voxel-Based Analysis of Regional Brain [^{11}C](+)McN-5652 Distribution Volumes Negatively Associated With Aggression Questionnaire Scores in 12 Methamphetamine Abusers*

	Cluster-Level Analysis		Voxel-Level Analysis		Talairach Coordinates		
Location	Corrected *P* Value	Voxels, No.	Corrected *P* Value	*z* Score	x	y	z
Right orbitofrontal cortex	<.001	20	.007	5.49	6	26	−21
Left inferior temporal cortex	<.001	38	.007	5.48	−57	−30	−19
Left orbitofrontal cortex	.001	10	.02	5.17	−10	34	−24
Right anterior cingulate cortex	<.001	12	.03	5.13	10	49	10

Abbreviation: [^{11}C](+)McN-5652, *trans*-1,2,3,5,6,10-beta-hexahydro-6-[4-(methylthio)phenyl]pyrrolo-[2,1-a]isoquinoline.
*The significance threshold was $P<.05$ at the corrected voxel level and $P<.05$ at the corrected cluster level. Coordinates are given in millimeters from the origin at the midpoint of the anterior commissure for voxels of peak significance.

based interviews. Furthermore, in this study, the severity of aggression clearly paralleled the decreases in serotonin transporter density in the brain, which in turn were found to be associated with the duration of methamphetamine use. Therefore, it seems unlikely that the increased aggression observed in these methamphetamine abusers reflected a preexisting disposition or personality trait.

Except for the scores on the AQ, none of the scores on the clinical rating scales for psychiatric symptoms were correlated with the decrease in serotonin transporter density. Methamphetamine has been reported to affect not only serotonergic neurons but also several other types of neurons, such as the dopaminergic, glutamatergic, and γ-aminobutyric acid (GABA)–ergic neurons, all of which have been implicated in the presence of a variety of psychiatric symptoms (eg, delusions, hallucinations, and anxiety).[63] It is possible that changes in various types of neurons might have affected or modified the clinical symptoms evaluated herein. Another plausible interpretation for the negative results is that, as seen in Table 1, the severity of most of the residual symptoms assessed in this study ranged from mild to moderate, and the variances of their distributions were relatively small; together, these factors may have biased the results toward the null hypothesis.

Herein, we recruited methamphetamine abusers from the community; they were recreational abusers of methamphetamine only, and none of them had used other illicit drugs or had taken toxic or high doses of methamphetamine. Although our strategy allowed us to evaluate the pure effects of methamphetamine on the human brain, the findings may not be generalized to the broad population of methamphetamine abusers. However, the combined use of methamphetamine with other illicit drugs is infrequent in Japan, as indicated by Japanese National Police Agency records in 2002.[64] One reason for this is that cannabis, cocaine, and major illicit drugs other than methamphetamine are not widely distributed in Japan.[64] Furthermore, a national survey of 233 methamphetamine abusers reported that only 2.6% of the abusers had undergone methamphetamine intoxication,[65] suggesting that abusers of an overdose of methamphetamine are rare in Japan. Consequently, our findings are considered to be fairly generalizable to the population of methamphetamine abusers, at least in Japan.

In this study, all the methamphetamine abusers exhibited some psychopathologic symptoms, even in an abstinent state. To our knowledge, no previous studies have examined the incidence of psychopathologic abnormalities in abstinent methamphetamine abusers recruited from the general community. In a study by Wada and Fukui,[65] who investigated the psychopathologic characteristics of 233 abstinent methamphetamine abusers recruited from hospitals in Japan (the period of abstinence exceeded 1 month; the mean ± SD duration of methamphetamine use was 11.1 ± 7.9 years), almost all the abusers exhibited some psychopathologic symptoms, such as auditory hallucinations, delusions of reference/persecution, mood disturbances, anxiety, insomnia, irritability, impulsivity, and personality changes, including the antisocial personality type. Such observations cannot be applied to absti-

nent abusers in the community as a whole but may provide some support for the high occurrence of psychopathologic symptoms observed in this study. In Japan, most methamphetamine abusers take the substance intravenously,[8] whereas in a study[66] from the United States, approximately 90% of methamphetamine abusers had no history of intravenous or intramuscular injection of methamphetamine. Furthermore, a study by Domier and colleagues[66] revealed that among recently abstinent methamphetamine abusers who had discontinued its use for several months, the injecting abusers had a significantly higher incidence of psychopathologic symptoms than the noninjecting abusers. These results suggest that in Japan, the intravenous intake of methamphetamine could predispose its abusers to persistent psychiatric problems, even after the cessation of methamphetamine use. Nevertheless, it remains an important and unresolved issue whether a reduction in serotonin transporter could be expected to occur in abusers with no psychopathologic signs or symptoms. To verify our findings that methamphetamine abuse is linked to a reduction in brain serotonin transporters, which in turn underlies persistent psychopathologic symptoms, additional studies that also incorporate a group of methamphetamine abusers with no apparent psychopathologic problems are required.

Wilson and colleagues[67] examined serotonin concentrations in postmortem tissue samples from human brains with a history of long-term methamphetamine abuse, although they did not study serotonin transporters per se. They concluded that there were no substantial alterations in serotonin concentrations in the global brain except in the medial prefrontal cortex (Brodmann area 11: a reduction of 56% compared with controls) and in the orbitofrontal cortex (Brodmann area 12: a reduction of 61% compared with controls). These results seem to contradict our observation of reductions in serotonin transporters in widely distributed brain regions. The discrepancy between the results of that postmortem study and those of present study is puzzling. However, one possible explanation for this discrepancy could be related to differences in the pattern and amount of drug use between the samples.[1,16,17] In Western countries, methamphetamine abusers often use other drugs, mainly cocaine or cannabis[68-70]; however, no information is provided with respect to this issue in the study by Wilson and colleagues.[67] Because methamphetamine is more likely to produce neurotoxic effects in serotonergic neurons than either cocaine or cannabis,[71,72] methamphetamine abusers who use this drug only could have experienced more severe damage to serotonergic neurons than abusers who simultaneously use other drugs, such as cocaine or cannabis. Furthermore, similar to most methamphetamine abusers in Japan, those in this study intravenously injected the substance. The intravenous intake may further potentiate the neurotoxic effects of methamphetamine.

To our knowledge, this is the first study to demonstrate a severe and long-lasting reduction in the density of the serotonin transporter in the living brains of methamphetamine abusers. The observed decrease in serotonin transporter density was also found to be associated with elevated levels of aggression. The present findings, combined with the results of previous animal studies, suggest that those who abuse methamphetamine may be at substantial risk for severe serotonin neuronal damage in the brain, potentially leading to persistently elevated aggression, even in those in a currently abstinent state.

Submitted for Publication: September 21, 2004; final revision received April 30, 2005; accepted July 7, 2005.
Correspondence: Yoshimoto Sekine, MD, PhD, Department of Psychiatry and Neurology, Hamamatsu University School of Medicine, 1-20-1 Handayama, Hamamatsu, Shizuoka 431-3192 Japan (ysekine@hama-med.ac.jp).
Acknowledgment: This work was supported by a Grant-in-Aid for the Center of Excellence from the Ministry of Education, Culture, Sports, Science, and Technology, Tokyo, Japan; research grant 16A for nervous and mental disorders from the Ministry of Health, Labor, and Welfare, Tokyo; a grant for the research on serotonin from the Public Health Research Foundation/New Frontiers of Neurotransmitter Research, Tokyo; and the Stanley Foundation, Bethesda, Md.

REFERENCES

1. McCann UD, Wong DF, Yokoi F, Villemagne V, Dannals RF, Ricaurte GA. Reduced striatal dopamine transporter density in abstinent methamphetamine and methcathinone users: evidence from positron emission tomography studies with [^{11}C]WIN-35,428. *J Neurosci.* 1998;18:8417-8422.
2. Volkow ND, Chang L, Wang GJ, Fowler JS, Leonido-Yee M, Franceschi D, Sedler MJ, Gatley SJ, Hitzemann R, Ding YS, Logan J, Wong C, Miller EN. Association of dopamine transporter reduction with psychomotor impairment in methamphetamine abusers. *Am J Psychiatry.* 2001;158:377-382.
3. Sekine Y, Iyo M, Ouchi Y, Matsunaga T, Tsukada H, Okada H, Yoshikawa E, Futatsubashi M, Takei N, Mori N. Methamphetamine-related psychiatric symptoms and reduced brain dopamine transporters studied with PET. *Am J Psychiatry.* 2001;158:1206-1214.
4. Farrell M, Marsden J, Ali R, Ling W. Methamphetamine: drug use and psychoses becomes a major public health issue in the Asia Pacific region. *Addiction.* 2002;97:771-772.
5. Hall W, Hando J, Darke S, Ross J. Psychological morbidity and route of administration among amphetamine users in Sydney, Australia. *Addiction.* 1996;91:81-87.
6. London ED, Simon SL, Berman SM, Mandelkern MA, Lichtman AM, Bramen J, Shinn AK, Miotto K, Learn J, Dong Y, Matochik JA, Kurian V, Newton T, Woods R, Rawson R, Ling W. Mood disturbances and regional cerebral metabolic abnormalities in recently abstinent methamphetamine abusers. *Arch Gen Psychiatry.* 2004;61:73-84.
7. Seivewright N. Disorders relating to the use of amphetamine and cocaine. In: Gelder MG, Lopez-Ibor JJ, Andreasen N, eds. *New Oxford Textbook of Psychiatry.* New York, NY: Oxford University Press; 2000:531-534.
8. Konuma K. Use and abuse of amphetamines in Japan. In: Cho AK, Segal DS, eds. *Amphetamine and Its Analogs.* San Diego, Calif: Academic Press; 1994:415-435.
9. Sekine Y, Minabe Y, Kawai M, Suzuki K, Iyo M, Isoda H, Sakahara H, Ashby CR Jr, Takei N, Mori N. Metabolite alterations in basal ganglia associated with methamphetamine-related psychiatric symptoms: a proton MRS study. *Neuropsychopharmacology.* 2002;27:453-461.
10. Sato M, Chen CC, Akiyama K, Otsuki S. Acute exacerbation of paranoid psychotic state after long-term abstinence in patients with previous methamphetamine psychosis. *Biol Psychiatry.* 1983;18:429-440.
11. Ricaurte GA, Schuster CR, Seiden LS. Long-term effects of repeated methylamphetamine administration on dopamine and serotonin neurons in the rat brain: a regional study. *Brain Res.* 1980;193:153-163.
12. Davidson C, Gow AJ, Lee TH, Ellinwood EH. Methamphetamine neurotoxicity: necrotic and apoptotic mechanisms and relevance to human abuse and treatment. *Brain Res Brain Res Rev.* 2001;36:1-22.
13. Matsuzaki H, Namikawa K, Kiyama H, Mori N, Sato K. Brain-derived neurotrophic factor rescues neuronal death induced by methamphetamine. *Biol Psychiatry.* 2004;55:52-60.

14. Ricaurte GA, Sabol KE, Seiden LS. Functional consequences of neurotoxic amphetamine exposure. In: Cho AK, Segal DS, eds. *Amphetamine and Its Analogs.* San Diego, Calif: Academic Press; 1994:297-313.
15. Kita T, Wagner GC, Nakashima T. Current research on methamphetamine-induced neurotoxicity: animal models of monoamine disruption. *J Pharmacol Sci.* 2003;92:178-195.
16. Villemagne V, Yuan J, Wong DF, Dannals RF, Hatzidimitriou G, Mathews WB, Ravert HT, Musachio J, McCann UD, Ricaurte GA. Brain dopamine neurotoxicity in baboons treated with doses of methamphetamine comparable to those recreationally abused by humans: evidence from [^{11}C]WIN-35,428 positron emission tomography studies and direct in vitro determinations. *J Neurosci.* 1998; 18:419-427.
17. Volkow ND, Chang L, Wang GJ, Fowler JS, Franceschi D, Sedler M, Gatley SJ, Miller E, Hitzemann R, Ding YS, Logan J. Loss of dopamine transporters in methamphetamine abusers recovers with protracted abstinence. *J Neurosci.* 2001; 21:9414-9418.
18. Sekine Y, Minabe Y, Ouchi Y, Takei N, Iyo M, Nakamura K, Suzuki K, Tsukada H, Okada H, Yoshikawa E, Futatsubashi M, Mori N. Association of dopamine transporter loss in the orbitofrontal and dorsolateral prefrontal cortices with methamphetamine-related psychiatric symptoms. *Am J Psychiatry.* 2003;160:1699-1701.
19. McCann UD, Szabo Z, Scheffel U, Dannals RF, Ricaurte GA. Positron emission tomographic evidence of toxic effect of MDMA ("Ecstasy") on brain serotonin neurons in human beings. *Lancet.* 1998;352:1433-1437.
20. Reneman L, Lavalaye J, Schmand B, de Wolff FA, van den Brink W, den Heeten GJ, Booij J. Cortical serotonin transporter density and verbal memory in individuals who stopped using 3,4-methylenedioxymethamphetamine (MDMA or "ecstasy"): preliminary findings. *Arch Gen Psychiatry.* 2001;58:901-906.
21. Szabo Z, McCann UD, Wilson AA, Scheffel U, Owonikoko T, Mathews WB, Ravert HT, Hilton J, Dannals RF, Ricaurte GA. Comparison of (+)-(11)C-McN5652 and (11)C-DASB as serotonin transporter radioligands under various experimental conditions. *J Nucl Med.* 2002;43:678-692.
22. Semple DM, Ebmeier KP, Glabus MF, O'Carroll RE, Johnstone EC. Reduced in vivo binding to the serotonin transporter in the cerebral cortex of MDMA ("ecstasy") users. *Br J Psychiatry.* 1999;175:63-69.
23. Scheffel U, Szabo Z, Mathews WB, Finley PA, Yuan J, Callahan B, Hatzidimitriou G, Dannals RF, Ravert HT, Ricaurte GA. Fenfluramine-induced loss of serotonin transporters in baboon brain visualized with PET. *Synapse.* 1996;24:395-398.
24. Bengel D, Isaacs KR, Heils A, Lesch KP, Murphy DL. The appetite suppressant d-fenfluramine induces apoptosis in human serotonergic cells. *Neuroreport.* 1998; 9:2989-2993.
25. McCann UD, Yuan J, Ricaurte GA. Neurotoxic effects of +/–fenfluramine and phentermine, alone and in combination, on monoamine neurons in the mouse brain. *Synapse.* 1998;30:239-246.
26. Poole R, Brabbins C. Drug induced psychosis. *Br J Psychiatry.* 1996;168:135-138.
27. Takebayashi K, Sekine Y, Takei N, Minabe Y, Isoda H, Takeda H, Nishimura K, Nakamura K, Suzuki K, Iwata Y, Sakahara H, Mori N. Metabolite alterations in basal ganglia associated with psychiatric symptoms of abstinent toluene users: a proton MRS study. *Neuropsychopharmacology.* 2004;29:1019-1026.
28. American Psychiatric Association. *Diagnostic and Statistical Manual of Mental Disorders, Fourth Edition.* Washington, DC: American Psychiatric Press; 1994.
29. First MB, Spitzer RL, Gibbon M, Williams JBW. *Structured Clinical Interview for the Diagnostic and Statistical Manual of Mental Disorders, Fourth Edition, Patient Version.* Washington, DC: American Psychiatric Press; 1997.
30. Al-Dirbashi OY, Kuroda N, Wada M, Takahashi M, Nakashima K. Quantification of methamphetamine, amphetamine and enantiomers by semi-micro column HPLC with fluorescence detection; applications on abusers' single hair analyses. *Biomed Chromatogr.* 2000;14:293-300.
31. Buss AH, Perry M. The aggression questionnaire. *J Pers Soc Psychol.* 1992;63: 452-459.
32. Hamilton M. The assessment of anxiety states by rating. *Br J Med Psychol.* 1959; 32:50-55.
33. Hamilton M. Development of a rating scale for primary depressive illness. *Br J Soc Clin Psychol.* 1967;6:278-296.
34. Mohr P, Horacek J, Motlova L, Libiger J, Czobor P. Prolactin response to D-fenfluramine challenge test as a predictor of treatment response to haloperidol in acute schizophrenia. *Schizophr Res.* 1998;30:91-99.
35. Overall JE, Gorham DR. The Brief Psychiatric Rating Scale. *Psychol Rep.* 1962; 10:799-812.
36. Volkow ND, Wang GJ, Fischman MW, Foltin RW, Fowler JS, Abumrad NN, Vitkun S, Logan J, Gatley SJ, Pappas N, Hitzemann R, Shea CE. Relationship between subjective effects of cocaine and dopamine transporter occupancy. *Nature.* 1997;386:827-830.
37. Ouchi Y, Nobezawa S, Okada H, Yoshikawa E, Futatsubashi M, Kaneko M. Altered glucose metabolism in the hippocampal head in memory impairment. *Neurology.* 1998;51:136-142.
38. Watanabe M, Shimizu K, Omura T, Takahashi M, Kosugi T, Yoshikawa E, Sato N, Okada H, Yamashita T. A new high resolution PET scanner dedicated to brain research. *IEEE Trans Nucl Sci.* 2002;49:634-639.
39. Parsey RV, Kegeles LS, Hwang DR, Simpson N, Abi-Dargham A, Mawlawi O, Slifstein M, Van Heertum RL, Mann JJ, Laruelle M. In vivo quantification of brain serotonin transporters in humans using [^{11}C]McN 5652. *J Nucl Med.* 2000; 41:1465-1477.
40. Ouchi Y, Yoshikawa E, Okada H, Futatsubashi M, Sekine Y, Iyo M, Sakamoto M. Alterations in binding site density of dopamine transporter in the striatum, orbitofrontal cortex, and amygdala in early Parkinson's disease: compartment analysis for β-CFT binding with positron emission tomography. *Ann Neurol.* 1999; 45:601-610.
41. Brody AL, Mandelkern MA, London ED, Childress AR, Lee GS, Bota RG, Ho ML, Saxena S, Baxter LR Jr, Madsen D, Jarvik ME. Brain metabolic changes during cigarette craving. *Arch Gen Psychiatry.* 2002;59:1162-1172.
42. Ouchi Y, Nobezawa S, Yoshikawa E, Futatsubashi M, Kanno T, Okada H, Torizuka T, Nakayama T, Tanaka K. Postural effects on brain hemodynamics in unilateral cerebral artery occlusive disease: a positron emission tomography study. *J Cereb Blood Flow Metab.* 2001;21:1058-1066.
43. Ouchi Y, Okada H, Yoshikawa E, Futatsubashi M, Nobezawa S. Absolute changes in regional cerebral blood flow in association with upright posture in humans: an orthostatic PET study. *J Nucl Med.* 2001;42:707-712.
44. Simpson HB, Lombardo I, Slifstein M, Huang HY, Hwang DR, Abi-Dargham A, Liebowitz MR, Laruelle M. Serotonin transporters in obsessive-compulsive disorder: a positron emission tomography study with [^{11}C]McN 5652. *Biol Psychiatry.* 2003;54:1414-1421.
45. Mikolajczyk K, Szabatin M, Rudnicki P, Grodzki M, Burger CA. JAVA environment for medical image data analysis: initial application for brain PET quantitation. *Med Inform (Lond).* 1998;23:207-214.
46. Tauscher J, Kapur S, Verhoeff NP, Hussey DF, Daskalakis ZJ, Tauscher-Wisniewski S, Wilson AA, Houle S, Kasper S, Zipursky RB. Brain serotonin 5-HT (1A) receptor binding in schizophrenia measured by positron emission tomography and [^{11}C]WAY-100635. *Arch Gen Psychiatry.* 2002;59:514-520.
47. Talairach J, Tournoux P. *Co-planer Stereotaxic Atlas of the Human Brain: 3-Dimensional Proportional System: An Approach to Cerebral Imaging.* Stuttgart, Germany: Georg Thieme; 1988.
48. Ito K, Morrish PK, Rakshi JS, Uema T, Ashburner J, Bailey DL, Friston KJ, Brooks DJ. Statistical parametric mapping with ^{18}F-dopa PET shows bilaterally reduced striatal and nigral dopaminergic function in early Parkinson's disease. *J Neurol Neurosurg Psychiatry.* 1999;66:754-758.
49. Ouchi Y, Kanno T, Okada H, Yoshikawa E, Futatsubashi M, Nobezawa S, Torizuka T, Tanaka K. Changes in dopamine availability in the nigrostriatal and mesocortical dopaminergic systems by gait in Parkinson's disease. *Brain.* 2001; 124:784-792.
50. Wang GJ, Volkow ND, Chang L, Miller E, Sedler M, Hitzemann R, Zhu W, Logan J, Ma Y, Fowler JS. Partial recovery of brain metabolism in methamphetamine abusers after protracted abstinence. *Am J Psychiatry.* 2004;161:242-248.
51. Kovachich GB, Aronson CE, Brunswick DJ. Effects of high-dose methamphetamine administration on serotonin uptake sites in rat brain measured using [^{3}H]cyanoimipramine autoradiography. *Brain Res.* 1989;505:123-129.
52. Davidson RJ, Putnam KM, Larson CL. Dysfunction in the neural circuitry of emotion regulation: a possible prelude to violence. *Science.* 2000;289:591-594.
53. Coccaro EF, Kavoussi RJ, Hauger RL, Cooper TB, Ferris CF. Cerebrospinal fluid vasopressin levels: correlates with aggression and serotonin function in personality-disordered subjects. *Arch Gen Psychiatry.* 1998;55:708-714.
54. Coccaro EF. Central serotonin and impulsive aggression. *Br J Psychiatry Suppl.* 1989;8:52-62.
55. Virkkunen M, Rawlings R, Tokola R, Poland RE, Guidotti A, Nemeroff C, Bissette G, Kalogeras K, Karonen SL, Linnoila M. CSF biochemistries, glucose metabolism, and diurnal activity rhythms in alcoholic, violent offenders, fire setters, and healthy volunteers. *Arch Gen Psychiatry.* 1994;51:20-27.
56. Linnoila M, DeJong J, Virkkunen M. Monoamines, glucose metabolism, and impulse control. *Psychopharmacol Bull.* 1989;25:404-406.
57. Roy A, Adinoff B, Linnoila M. Acting out hostility in normal volunteers: negative correlation with levels of 5HIAA in cerebrospinal fluid. *Psychiatry Res.* 1988; 24:187-194.
58. Linnoila M, Virkkunen M, Scheinin M, Nuutila A, Rimon R, Goodwin FK. Low cerebrospinal fluid 5-hydroxyindoleacetic acid concentration differentiates impulsive from nonimpulsive violent behavior. *Life Sci.* 1983;33:2609-2614.
59. Grafman J, Schwab K, Warden D, Pridgen A, Brown HR, Salazar AM. Frontal lobe injuries, violence, and aggression: a report of the Vietnam Head Injury Study. *Neurology.* 1996;46:1231-1238.
60. Parsey RV, Oquendo MA, Simpson NR, Ogden RT, Van Heertum R, Arango V, Mann JJ. Effects of sex, age, and aggressive traits in man on brain serotonin

5-HT_{1A} receptor binding potential measured by PET using [C-11]WAY-100635. *Brain Res.* 2002;954:173-182.
61. Lai MK, Tsang SW, Francis PT, Esiri MM, Keene J, Hope T, Chen CP. Reduced serotonin 5-HT_{1A} receptor binding in the temporal cortex correlates with aggressive behavior in Alzheimer disease. *Brain Res.* 2003;974:82-87.
62. van den Bree MB, Svikis DS, Pickens RW. Genetic influences in antisocial personality and drug use disorders. *Drug Alcohol Depend.* 1998;49:177-187.
63. Wrona MZ, Yang Z, Zhang F, Dryhurst G. Potential new insights into the molecular mechanisms of methamphetamine-induced neurodegeneration. *NIDA Res Monogr.* 1997;173:146-174.
64. National Police Agency (Japan). *Criminal White Paper* [in Japanese]. Tokyo, Japan: Printing Bureau, Ministry of Finance of Japan; 2004.
65. Wada K, Fukui S. Relationship between years of methamphetamine use and symptoms of methamphetamine psychosis [in Japanese]. *Arukoru Kenkyuto Yakubutsu Ison.* 1990;25:143-158.
66. Domier CP, Simon SL, Rawson RA, Huber A, Ling W. A comparison of injecting and noninjecting methamphetamine users. *J Psychoactive Drugs.* 2000;32:229-232.
67. Wilson JM, Kalasinsky KS, Levey AI, Bergeron C, Reiber G, Anthony RM, Schmunk GA, Shannak K, Haycock JW, Kish SJ. Striatal dopamine nerve terminal markers in human, chronic methamphetamine users. *Nat Med.* 1996;2:699-703.
68. Richter KP, Ahluwalia HK, Mosier MC, Nazir N, Ahluwalia JS. A population-based study of cigarette smoking among illicit drug users in the United States. *Addiction.* 2002;97:861-869.
69. Sumnall HR, Wagstaff GF, Cole JC. Self-reported psychopathology in polydrug users. *J Psychopharmacol.* 2004;18:75-82.
70. Smart RG, Mann RE, Tyson LA. Drugs and violence among Ontario students. *J Psychoactive Drugs.* 1997;29:369-373.
71. Jacobsen LK, Staley JK, Malison RT, Zoghbi SS, Seibyl JP, Kosten TR, Innis RB. Elevated central serotonin transporter binding availability in acutely abstinent cocaine-dependent patients. *Am J Psychiatry.* 2000;157:1134-1140.
72. Croft RJ, Klugman A, Baldeweg T, Gruzelier JH. Electrophysiological evidence of serotonergic impairment in long-term MDMA ("ecstasy") users. *Am J Psychiatry.* 2001;158:1687-1692.

Clinical Trials Registration

In concert with the International Committee of Medical Journal Editors, *Archives of General Psychiatry* will require, as a condition of consideration for publication, registration of clinical trials in a public trials registry (such as http://ClinicalTrials.gov or http://controlled-trials.com). Trials must be registered at or before the onset of patient enrollment. This policy applies to any clinical trial starting enrollment after March 1, 2006. For trials that began enrollment before this date, registration will be required by June 1, 2006. The trial registration number should be supplied at the time of submission.

For details about this new policy see the editorials by DeAngelis et al in the September 8, 2004 (2004;292:1363-1364) and June 15, 2005(2005;293:2927-2929) issues of *JAMA*.

ELSEVIER

NeuroImage

www.elsevier.com/locate/ynimg
NeuroImage 29 (2006) 697 – 705

Cerebral hemodynamics evaluation by near-infrared time-resolved spectroscopy: Correlation with simultaneous positron emission tomography measurements

Etsuko Ohmae,[a,*] Yasuomi Ouchi,[b] Motoki Oda,[a] Toshihiko Suzuki,[a] Shuji Nobesawa,[b] Toshihiko Kanno,[b] Etsuji Yoshikawa,[a] Masami Futatsubashi,[a] Yukio Ueda,[a] Hiroyuki Okada,[a] and Yutaka Yamashita[a]

[a]*Central Research Laboratory, Hamamatsu Photonics K.K., 5000 Hirakuchi, Hamamatsu, Shizuoka 434-8601, Japan*
[b]*Positron Medical Center, Hamamatsu Medical Center, 5000 Hirakuchi, Hamamatsu, Shizuoka 434-0041, Japan*

Received 18 August 2004; revised 3 March 2005; accepted 4 August 2005
Available online 13 September 2005

We compared pharmacologically-perturbed hemodynamic parameters (cerebral blood volume; CBV, and flow; CBF) by acetazolamide administration in six healthy human subjects studied with positron emission tomography (PET) and near-infrared (NIR) time-resolved spectroscopy (TRS) simultaneously to investigate whether NIR-TRS could measure in vivo hemodynamics in the brain tissue quantitatively. Simultaneously with the PET measurements, TRS measurements were performed at the forehead with four different optode spacing from 2 cm to 5 cm. Total hemoglobin and oxygen saturation (SO_2) measured by TRS significantly increased after administration of acetazolamide at any optode spacing in all subjects. In PET study, CBV and CBF were estimated in the following three volumes of interest (VOIs) determined on magnetic resonance images, VOI_1: scalp and skull, VOI_2: gray matter region, VOI_3: gray and white matter regions. Acetazolamide treatment elevated CBF and CBV significantly in VOI_2 and VOI_3 but VOI_1. TRS-derived CBV was more strongly correlated with PET-derived counterpart in VOI_2 and VOI_3 when the optode spacing was above 4 cm, although optical signal from cerebral tissue could be caught with any optode spacing. As to increase of the CBV, 4 cm of optode spacing correlated best with VOI_2. To support the result of TRS-PET experiment, we also estimated the contribution ratios of intracerebral tissue to observed absorption change based on diffusion theory. The contribution ratios at 4 cm were estimated as follows: 761 nm: 50%, 791 nm: 72%, 836 nm: 70%. These results demonstrated that NIR-TRS with 4 cm of optode spacing could measure cerebral hemodynamic responses optimally and quantitatively.

Introduction

Near-infrared spectroscopy (NIRS) allows simple, non-invasive measurement of the oxygenation state and hemodynamics in living tissue by utilizing the differential in absorption spectrum between oxygenated and deoxygenated hemoglobin. This field got its start from the finding by Jobsis (1977) that when a cat's head is irradiated with near-infrared (NIR) light, the intensity of the transmitted light shows changes according to the oxygen metabolic state in the tissues. Since then, there has been growing study and technique of NIRS measurement.

Making that advantage, this method has been expected for use in surgical operations (Kakihana et al., 1996; De Blasi et al., 1997) and neonate respiration care (Meek et al., 1999; Isobe et al., 2000). Besides the clinical field, topographical imaging by multi-channels measurement is being performed to observe brain activity on the cortex (Watanabe et al., 2000; Tanosaki et al., 2001).

NIRS encompasses some different techniques and analysis, and we are adopting approaches of time-resolved spectroscopy (TRS; Oda et al., 1996; Yamashita et al., 1998), phase modulated spectroscopy (PMS; Tuchiya and Urakami, 1996; Iwai et al., 2001) or spatially resolves spectroscopy (SRS; Suzuki et al., 1999) method, etc. to quantification.

In contrast to the wide applicability of NIRS to brain monitoring, fundamental and critical questions still remain to be clarified, one of which is light propagation in the human head. The effect of the various external tissues of the head such as skin, skull and cerebrospinal fluid (CSF) on photon propagation in the internal cerebral tissue has not yet been fully examined in vivo.

Several researchers (Firbank et al., 1995; Okada et al., 1997) expressed doubts about the use of NIRS on adult human heads due to problems from the multi-layered structure of the scalp, skull, CSF and the cerebral tissue. Firbank first showed that the presence of CSF had a significant effect on the light distribution. It was

* Corresponding author. Fax: +81 53 586 6180.
E-mail address: etuko-o@crl.hpk.co.jp (E. Ohmae).
Available online on ScienceDirect (www.sciencedirect.com).

1053-8119/$ - see front matter © 2005 Elsevier Inc. All rights reserved.
doi:10.1016/j.neuroimage.2005.08.008

reported that the NIRS signal from the adult human head was only 10–20% of the total signal due to the effect of CSF from the Monte Carlo simulation. These doubts are related to the essential question of where to measure using the photon, and research studies are being conducted using both simulations (Okada and Delpy, 2000, 2003a,b; Misonoo and Okada, 2001) and experimental measurements. On the contrary, several researchers (McCormick et al., 1992; Harris et al., 1994; Germon et al., 1995; Kohri et al., 2001) have reported that NIRS can detect the brain signals more specifically by increasing the optode spacing from experimental measurements.

In this study, in order to investigate the relation between the optode spacing and light sampling depth, we observed change in the cerebral blood volume (CBV) of six adult subjects by administration of a drug with simultaneous measurement of the TRS system which can measure the blood volume and the oxygen saturation (SO_2) quantitatively and positron emission tomography (PET), and we compared the CBV by TRS (TRS CBV) with CBV by PET (PET CBV) and estimated the contribution ratios of intracerebral tissue to the observed absorption change at three different wavelengths.

Materials and methods

Subjects

Six healthy male subjects (mean age, 42.6 ± 5.08; range, 37 to 51 years) were studied. Informed consent was obtained from all subjects before experiment. It was confirmed that they had no previous history of intracranial disorders and also that there were no anatomical abnormalities by making a check with a magnetic resonance imaging (MRI; 0.3 T MRP7000AD, Hitachi Ltd., Japan).

Three-wavelength TRS system

We used TRS-10 system (Hamamatsu Photonics K.K., Japan) (Oda et al., 2000) to obtain TRS-CBV in our experiment. This system uses time-correlate single photon counting (TCPC) method for measuring the temporal function of the sample. The system measures the intensity of light in a time domain and enables analysis of to the data with the time domain photo diffusion equation (Patterson et al., 1989). The block diagram of this system is shown in Fig. 1.

As the light source, this system uses semiconductor lasers called "Picosecond Light Pulser (PLP, Hamamatsu Photonics K.K., Japan)" emitting light pulses at three different wavelengths (761 nm, 791 nm, 836 nm) with a peak power of 60 mW, average power of 30 μW, the full with at half maximum (FMHM) of 100 ps and repetition frequency of 5 MHz. The detector section of this system consists of a photomultiplier tube (PMT, H6279-MOD, Hamamatsu Photonics K.K., Japan) followed by constant fraction discriminators (CFD), time-to-amplitude converters (TAC), A/D converters and histogram memories.

The system instrumental function is about 160 ps FMWH. The three PLPs emit light pulses on a time series, and the 3-wavelength optical pulses (761, 791, 836 nm) are guided into one optical fiber via a fiber coupler (CH20G-D3-CF, Mitsubishi Gas Chemical Company Inc., Japan). An optical switch (SC SERIES, JDS FITEL Inc., Canada) in this experiment selected the light irradiation point. A neutral density filter installed between the optical switch and each irradiation fiber maintained the light entering the PMT at a correct level. Each single optical fiber (GC200/250L, FUJIKURA Ltd., Japan) used for light irradiation has a numerical aperture (N.A.) of 0.25 and a core diameter of 200 μm. The optical bundle fiber (LB21E, HOYA Corp., Japan) used to collect the light has an N.A. of 0.21 and a bundle diameter of 3 mm.

TRS data analysis

The observed temporal profiles were fitted into the photon diffusion equation (Patterson et al., 1989) using the non-linear least square fitting method. The reduced scattering (μ_s') and absorption coefficients (μ_a) for three wavelengths were calculated (Appendix A). Then oxyhemoglobin (TRS HbO_2), deoxyhemoglobin (TRS Hb), total hemoglobin (TRS tHb) and oxygen saturation (SO_2) were calculated with least square method (Appendix B). We then converted the TRS tHb into the TRS CBV for comparison with the PET CBV (Appendix C). Additionally, we calculated the partial mean pathlength of extracerebral tissue (L_{ext}) at each wavelength

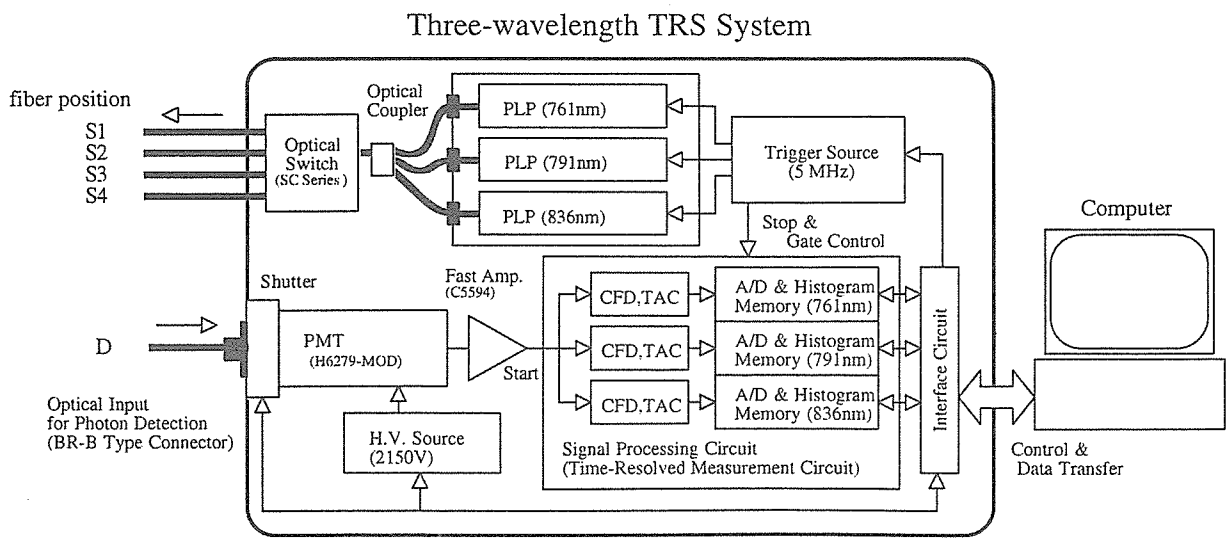

Fig. 1. Block diagram of time-resolved spectroscopy system (TRS-10: Hamamatsu Photonics K.K.).

by applying the method by the reference (Kohri et al., 2001) for five subjects whose absorption coefficients (μ_a) increased proportional to optode spacing from 2 to 4 cm. The observed mean pathlength (L_{obs}) was calculated (Zhang et al., 1998) from temporal profiles. Then, we determined the contribution ratio of the intracerebral tissue to the observed absorption change using these values.

TRS fiber position

Prior to the experiment, headgear was made for each volunteer to fix the TRS optical fibers to their left forehead. The headgear was made of thermoplastic material (ESS-15, Engineering System Co., Japan) to ensure a secure fit onto the head of each volunteer. A total of five fiber holders were fabricated for four light irradiation points (S_{1-4}) with optode spacings of 2, 3, 4 and 5 cm and one light detection point (D), and a black sheet was affixed to the inner side of the headgear except for the fiber holders to shield a detection fiber from stray light propagating on the skin surface. More specifically, the light irradiation point S_4 was first established on the left forehead, at a point 35 mm above supra-orbital margin so as to avoid the frontal sinus, and also 1 cm away from the median line to avoid the superior sagittal sinus. Next, the other light irradiation and detection points (S_{1-3}, D) were established using this point (S_4) as a reference. The positions of the light irradiation and detection points (S_{1-4}, D) on the MRI image of the head are shown in Fig. 2A. After measurement was complete, the value of optode spacing for substitution into the photon diffusion equation was measured as a straight distance with calipers. Fabricating headgear allowed the measurement to be easily made and permitted setting accurate optode spacing.

PET procedure

PET was performed using a high resolution PET scanner (SHR22000, Hamamatsu Photonics KK, Hamamatsu, Japan) (Iwase et al., 2002) with spatial resolution of 3.6 mm at full width half maximum (FWHM) transaxially and 4.2 mm axially, and with a 23-cm axial field of view, yielding 63 image slices simultaneously. After backprojection and filtering, the image resolution was 8.0 × 8.0 × 5.3 mm FWHM. The voxel of each reconstructed image measured 1.73 × 1.73 × 3.6 mm. Just prior to PET measurement, each subject underwent an MRI for determining the brain scanning area by using a static magnet with 3-dimensional mode acquisition (Ouchi et al., 1998). Fifteen-minute transmission scan for attenuation correction was performed with a $^{68}Ge/^{68}Ga$ source.

We applied the ^{15}O-CO short inhalation method followed by 5 min of data acquisition to measure the PET CBV (Lammertsma and Jones, 1983; Lammertsma et al., 1987). During this acquisition period, two pairs of arterial blood samples were collected for determining arterial ^{15}O-CO radioactivity.

One hundred twenty-second dynamic emission scans (10 s × 12 frames) were performed while subjects received a 500-MBq bolus of $H_2^{15}O$ through the right cubital vein by an automated injector. Simultaneously after injection, arterial blood was continuously withdrawn through the left brachial artery using the automated arterial blood γ-ray coincidence counter (BACC-2: Hamamatsu Photonics K.K., Hamamatsu, Japan) yielding arterial input data per second (Ouchi et al., 2001). A quantitative PET CBF value was estimated using 2-min $H_2^{15}O$ data accumulated after the tracer started circulating in the brain by summing the dynamic frames based on the autoradiographic method (Herscovitch et al., 1983).

Physiological parameters were monitored during PET examination and additional arterial blood samples were taken after each scan for analyzing levels of $PaCO_2$, Hb, hematocrit and arterial pH using a blood gas analyzer (Bayer Rapidlab 860, Tokyo, Japan). The psychophysical condition of each subject was evaluated by asking if any different sensation or mental activity was developed during the whole measurement in order to exclude any change in such brain activities as a confounding factor.

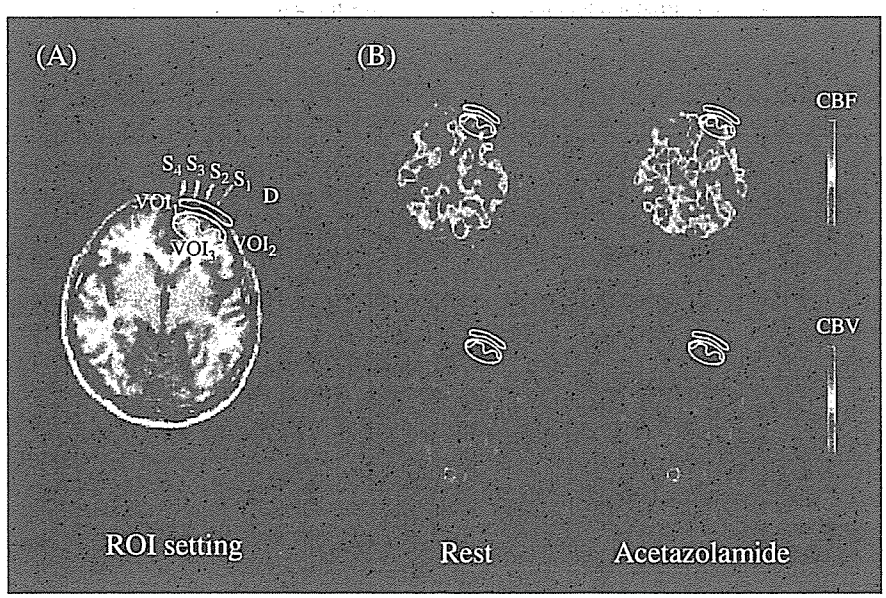

Fig. 2. Fiber and VOI positions setting on MRI image and PET images. (A) Fiber markers appear on left forehead. S_{1-4} and D are corresponding to irradiation fibers and a detection fiber, respectively. Optode spacings of S_1-D: 2 cm, S_2-D: 3 cm, S_3-D: 4 cm, S_4-D: 5 cm were set. The four PET VOIs were set as follows. VOI_1: extracerebral tissue, VOI_2: gray matter region, VOI_3: gray matter and white matter regions. (B) Images of typical measurements (41 years old; male) of PET CBF (upper) and PET CBV (lower) in the resting (left) and loading (right) state.

After measurements, to grasp the TRS light irradiation and detection points on the PET image, the fiber positions were marked by multi-modality radiographic markers (MM-3004, I.Z.I Medical Products Corp., USA) and the brain once again measured by MRI.

PET VOI

The volume of interest (VOI) on PET image used for comparison with TRS values was set by means of the following procedure. First of all, 3-dimensional MRI images were cut into 3.6 mm thick slices transversely along the multi-modality radiographic marker line. Then two slices involving these markers were selected from all these slices. Next, the following four VOIs were placed under S_4-D area on the two slices. These were set as VOI_1: extracerebral tissues (such as scalp and skull), VOI_2: gray matter region, VOI_3: gray matter and white matter regions. These VOIs were then repositioned on the PET image matching the selected two MRI slices as the PET VOIs. Mean values for each VOI size were VOI_1: 2.88 cm^3, VOI_2: 3.16 cm^3, VOI_3: 5.99 cm^3. The VOI settings are shown in Fig. 2A.

Since the PET CBF and PET CBV values were calculated with coefficients established for intracerebral tissues, the data of VOI_1 set in extracerebral tissues were treated with arbitrary unit.

Protocol

PET measurements were performed in the resting state (before administration) and the loading state (after administration) at more than 20 min after the intravenous administration of 1000 mg acetazolamide (Diamox, Japan Wyeth Ledele Ltd., Japan) appeared to be the maximum effect of cerebral vasodilatation. Two CBF measurements and one CBV measurement with PET were performed in resting and loading state.

In the TRS measurement, the optode spacings were changed in sequence by switching the four light irradiation points (S_{1-4}) with an optical switch. To maintain a peak count greater than 5000 (Suzuki et al., 1994), the acquisition times at each light irradiation point were set to 10, 20, 30 and 120 s. These TRS measurements were performed consecutively on a time series from the start to the finish of the PET measurements. Subjects were kept at rest while lying face up on the bed during measurements. The protocol is shown in Fig. 3.

Statistical analysis

All results were expressed as mean ± SD. Statistical significance of the changes in PET CBV, PET CBF, TRS CBV and SO_2 before and after administration of acetazolamide was analyzed by paired t test. Statistical significance of contribution ratio among wavelengths was analyzed by ANOVA and Bonferroni t test. A significant difference was defined when statistical probability: P was less than 0.05.

The association between TRS CBV and PET CBV was evaluated by squared Pearson's correlation coefficient (r^2). Change in CBV (ΔCBV) by administration of acetazolamide was also evaluated in the same way. The assessment for VOI_1 was not performed because it was expressed in the arbitrary unit. Statistical significance of r^2 was analyzed by a t test for r^2. A significant difference was defined when statistical probability: P was less than 0.05.

Results

Physiology

There were no significant changes in physiologic parameters (arterial blood pressure, pulse rates, $PaCO_2$) and psychophysical states (changes in mental activity) between before and after administration of acetazolamide (data is not shown).

TRS

Typical values of TRS tHb and SO_2 at each optode spacing during the experiment are shown in Fig. 4. The rise of TRS tHb and SO_2 was confirmed at all optode spacings immediately after administering acetazolamide and reached a plateau after about 10 min. These phenomena were observed in all subjects.

Mean values of TRS CBV and SO_2 at each optode spacing in the resting and loading states are shown in Fig. 5. The TRS CBV and SO_2 at each optode spacing in resting state were as follows: 2 cm: 2.7 ± 0.4 cm^3/100 g, 70.3 ± 1.1%, 3 cm: 3.0 ± 0.2 cm^3/100 g, 68.7 ± 1.8%, 4 cm: 3.0 ± 0.3 cm^3/100 g, 69.6 ± 2.3%, 5 cm: 2.7 ± 0.3 cm^3/100 g, 71.7 ± 2.8%. The TRS CBV and SO_2 in loading

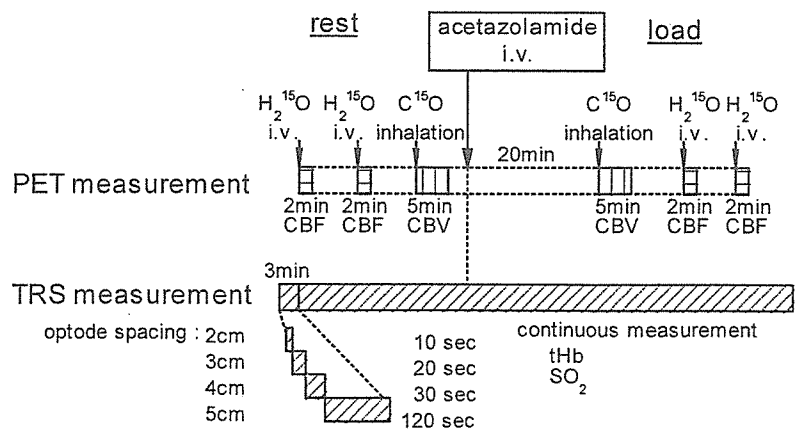

Fig. 3. TRS and PET simultaneous measurement protocol. The TRS measurement was made while switching the light irradiation point to set optode spacings of 2, 3, 4 and 5 cm. Data acquisition time was 10, 20, 30 and 120 s at each irradiation point. In the PET measurement, CBF was measured twice and CBV once, both resting and loading state. One CBF measurement required 2 min and the CBV measurement 5 min.

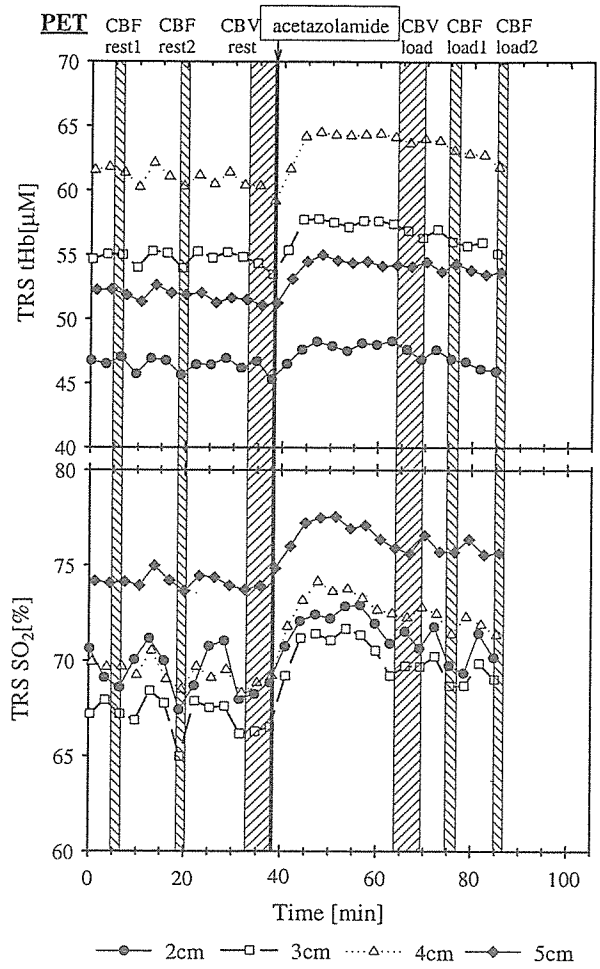

Fig. 4. TRS measurement results at each optode spacing. Typical responses (41 years old; male) of TRS tHb (upper) and SO_2 (lower) for acetazolamide administration. The oblique lines indicate PET data acquisition period.

state significantly rose approximately 6% and 3%, respectively, of resting state at all optode spacing.

PET

The CBF and CBV images at the resting and loading state are shown in Fig. 2B. The CBF can be clearly seen to increase after administering acetazolamide, whereas the CBV shows a relatively minor increase.

Mean values of PET CBF and PET CBV at each VOI in the rest and loading state are shown in Fig. 6. The PET CBF and PET CBV at each VOI in the resting state were as follows: VOI_1 (arbitrary unit): 6.6 ± 1.2 cm^3/100 g/min, 2.6 ± 0.4 cm^3/100 g, VOI_2: 39.6 ± 5.3 cm^3/100 g/min, 4.4 ± 0.9 cm^3/100 g, VOI_3: 40.6 ± 5.1 cm^3/100 g/min, 4.0 ± 0.7 cm^3/100 g. The PET CBF and PET CBV at $VOI_{2,3}$ in the loading state significantly increased approximately 30% and 10%, respectively, compared to those of resting state. However, no significant increases were observed for the CBF and CBV at VOI_1, which increased 8.2% and −1.3%, respectively.

Correlations

The r^2 for the CBV and ΔCBV, respectively, between TRS and PET are shown in Tables 1A and B.

The r^2 of CBV at 4 cm and 5 cm of optode spacing was higher than those at 2 cm and 3 cm of optode spacing at all VOI, and they also showed high correlation values as the depth increased.

As to ΔCBV, r^2 of VOI_2 showed exceptionally higher than those of VOI_3 at all optode spacing. At the VOI_2, however, r^2 at 2 cm of optode spacing showed lower than those at other optode spacing. At the VOI_3, just as with the CBV correlation, r^2 at 4 cm and 5 cm of optode spacing showed higher than those at 2 cm and 3 cm of optode spacing.

L_{ext} and the contribution ratio

L_{ext} at each wavelength was as follows: 761 nm 11.7 ± 2.7 cm, 791 nm: 6.3 ± 2.4 cm, 836 nm: 6.5 ± 1.5 cm. L_{ext} at 761 nm was significantly longer than those of 791 and 836 nm, against

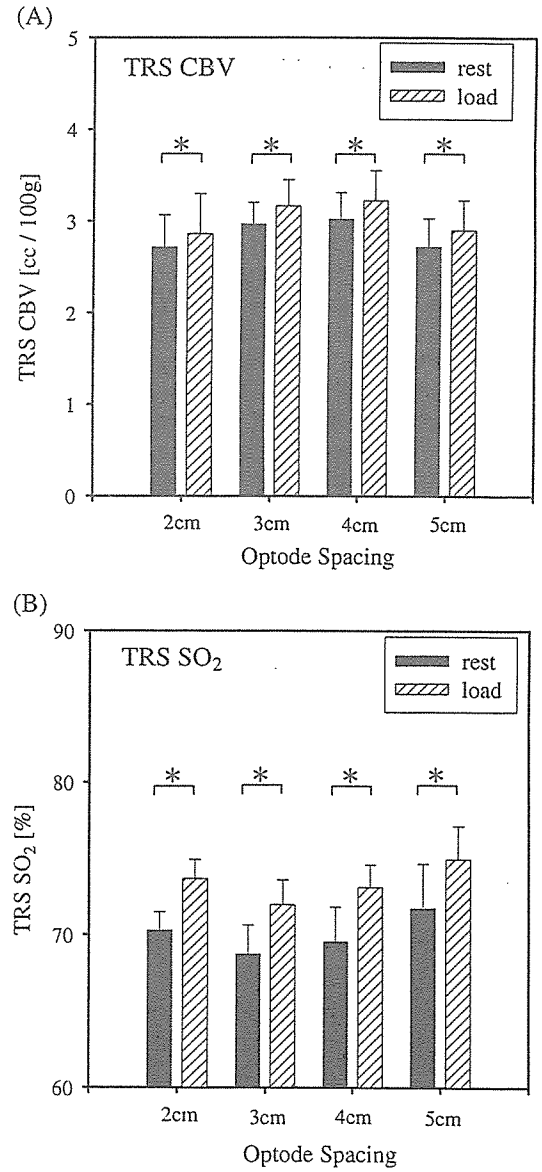

Fig. 5. Mean values (n = 6) for (A) TRS CBV and (B) SO_2 in the resting and loading state. Significant differences were confirmed for all optode spacings after administering acetazolamide (*P < 0.05).

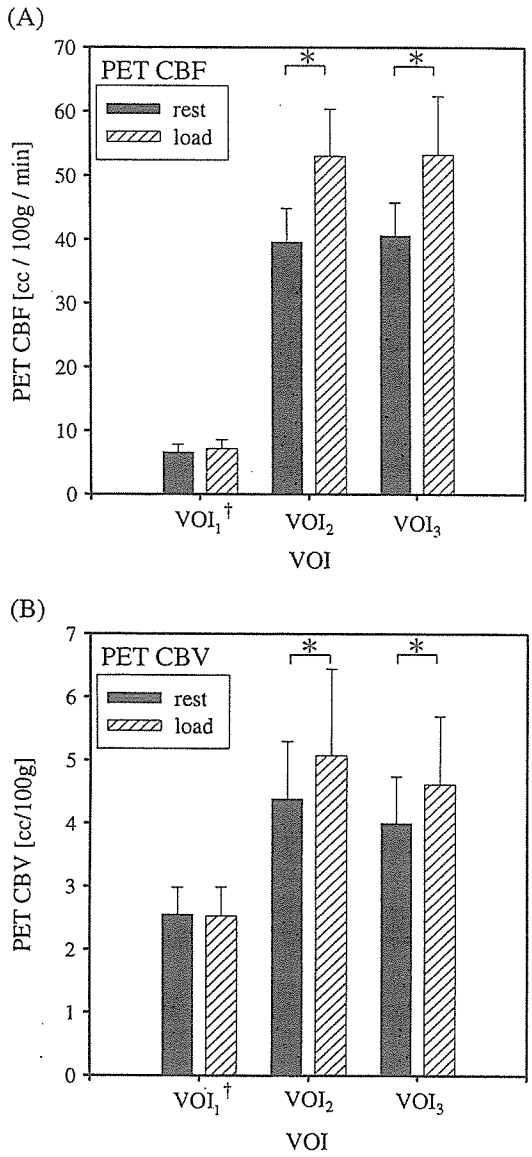

Fig. 6. Mean values (n = 6) for (A) PET CBF and (B) PET CBV in the resting and loading state. Significant differences were confirmed at VOI_2 and VOI_3 after administering acetazolamide (*P < 0.05). †VOI_1 was expressed in the arbitrary unit.

observed mean pathlength of each wavelengths were also the same (data is not shown).

The contribution ratios of the cerebral tissue at each wavelength are shown in Fig. 7. The contribution ratios of 761 nm with all optode spacing were significantly lower than those of 791 and 836 nm.

Discussion

The acetazolamide used in this experiment increases the regional CBF by inhibiting carbonic anhydrase and thereby expanding cerebral blood vessels (Posner and Plum, 1960; Ehrenreich et al., 1961). This drug is therefore generally used to assess the cerebrovascular reserve capacity as an acetazolamide test. Similarly in this study, significant increases of PET CBF and PET CBV by

Table 1
Squared correlation coefficient (r^2) between PET and TRS: (A) CBV; (B) ΔCBV

TRS optode spacing	PET	
	VOI_2	VOI_3
(A) r^2: TRS CBV vs. PET CBV (n = 6)		
2 cm	0.601**	0.535**
3 cm	0.410*	0.525**
4 cm	0.690**	0.841**
5 cm	0.762**	0.859**
(B) r^2: TRS ΔCBV vs. PET ΔCBV (n = 6)		
2 cm	0.331	0.050
3 cm	0.633*	0.277
4 cm	0.699*	0.457
5 cm	0.585	0.352

* $P < 0.05$.
** $P < 0.01$.

acetazolamide in the intracerebral tissues ($VOI_{2,3}$) and no significant increase of those in the extracerebral tissues (VOI_1) were confirmed. In the TRS measurements on the other hand, significant increases in CBV at all optode spacings were observed. Further, the result of significant increases of SO_2 at all optode spacing agrees well with a report (Vorstrup et al., 1984) that there was hardly any change in $CMRO_2$ even though the CBF increased when acetazolamide was administered. These results suggest that when optode spacing is 2 cm to 5 cm, the photons passing through the head convey the intracerebral hemodynamic response.

However, the CBV and ΔCBV correlations clearly differed according to the optode spacing and VOI. As for CBV correlation, these trends suggest that the longer the optode spacing, the deeper the region that the photons can penetrate, because the correlation with VOI_3 was higher than that with VOI_2 at each optode spacing except at 2 cm. In addition, correlations at 4 cm and 5 cm of optode spacing showed a trend to higher than those at 2 cm and 3 cm of optode spacing with both VOIs. These results suggested that optode spacing was preferably more than 4 cm for improving quantification of NIR-TRS to cerebral hemodynamics.

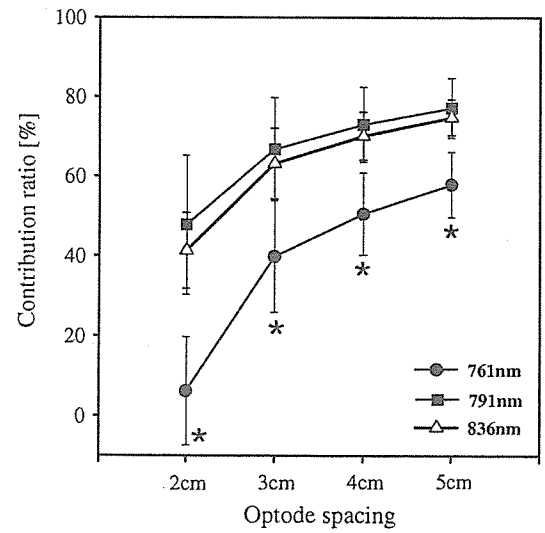

Fig. 7. Mean values (n = 5) for contribution rations of the cerebral tissue to observed absorption change. Significant differences were confirmed for all optode spacing at 761 nm to 791 and 836 nm (*P < 0.05).

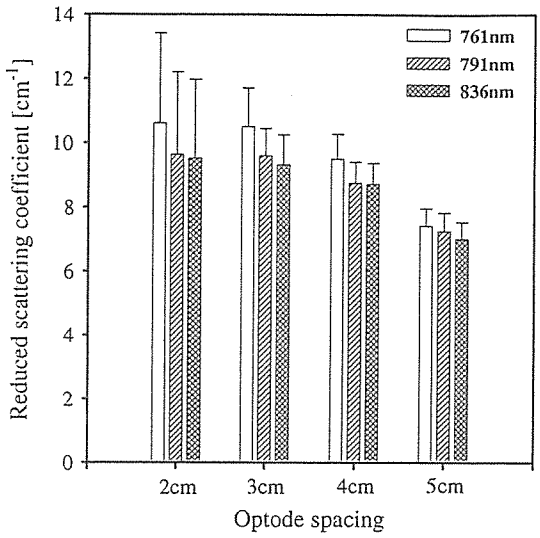

Fig. 8. Mean values (n = 5) for reduced scattering coefficient at each wavelength and optode spacing. The values of 761 nm for all optode spacing were highest among three wavelengths (no significant differences).

Because the density of blood vessels in VOI_2, which covers the gray matter mostly, was high, there might be a large increase in blood volume. Accordingly, the ΔCBV correlation with VOI_2 may be higher than VOI_3 regardless of the optode spacing. Also, the ΔCBV correlation for VOI_2 is a maximum at 4 cm of optode spacing so that this distance may be optimum for capturing cerebral hemodynamics response around the gray matter region.

Contribution ratios at 4 cm of optode spacing were as follows: 761 nm: 50.4 ± 10.3%, 791 nm: 72.9 ± 9.4%, 836 nm: 70.0 ± 6.0%. The results at 836 nm are very much in agreement with the results at 834 nm by Kohri (Kohri et al., 2001). But these results are different from previous simulation work (Firbank et al., 1995). The photon propagation depends heavily on the optical parameters of tissues. We believe that the μ_a and μ_s' of the postmortem adult human brain (Van der Zee et al., 1992) and piglet (Firbank et al., 1993) used in the simulation work maybe different from those in living tissues. Furthermore, both contribution ratios at 5 cm of optode spacing were higher than those at 4 cm and the ΔCBV correlation at 5 cm of optode spacing is lower than that at 4 cm; thus it is speculated that photons has penetrated even deeper, and contains information not only on gray matter but also on white matter and cerebral ventricle. Conversely, the lowest value of the ΔCBV correlation at 2 cm of optode spacing corresponds with derived low contribution ratios. So the 2 cm of optode spacing is not recommended for acquiring intracerebral information. Although we treated a complex layered structure as a single set of μ_a and μ_s', assuming of a homogeneous medium, making optode spacing longer could satisfy this condition concededly.

L_{ext} at 761 nm was 1.7 times of those at 791 and 836 nm, although observed mean pathlength at each wavelength was also the same values. It means that the photons of 761 nm are hard to penetrate into the cerebral tissue than those of 791 and 836 nm. To support this result, mean values for μ_s' at each wavelength and the optode spacing in the resting state are shown in Fig. 8. As the higher the scattering, the photons are harder to spread into the cerebral tissue deeply. The difference of μ_s' among wavelength showed a similar tendency to that of L_{ext}. It was also reported that the value of μ_s' increases progressively with decreasing wavelength (Bevilacqua et al., 1999; Torricelli et al., 2001). To improve the accuracy of NIR measurement, it should be necessary to consider wavelength selection including μ_s' as well as absorption spectra of hemoglobin.

The TRS system has a potential to quantitate the hemoglobin concentration since it directly measures the optical pathlength distribution of detected photons passing through the living tissue, different from the conventional measurement methods (Brazy et al., 1985; Ferrari et al., 1987; Cope and Delpy, 1988). This allows making patient-to-patient comparisons and comparing the patient condition before and after treatment, making it highly valuable as an indicator for diagnosis and treatment. In this study, a good correlation coefficient was obtained between TRS-derived CBV and PET-derived CBV, while the absolute CBV levels by TRS were lower than those by PET. One reason for the under-/over-estimation of the CBV values might be a difference in modalities which measure different in vivo responses. An absolute value of CBV weighs considerably in the NIRS study. Thus, further studies are needed to resolve this methodological issue.

NIR measurement is proven capable of continuous measurement with high time resolution while also being a simple, safe and non-invasive method. Additionally, study of diffuse optical tomography is being proceeded based on this technology (Ueda et al., 2001; Hillman et al., 2001). We hope to further develop our work in the NIRS field to the level where it can be used as a modality to assist and complement PET technology.

Conclusion

We observed a change in the CBV by administration of acetazolamide with simultaneous measurement of TRS and PET. These experiments showed that intracerebral hemodynamics response by administering acetazolamide could be captured at optode spacings of 2 cm to 5 cm.

Furthermore, by evaluating the correlation with PET, we concluded that more than 4 cm of optode spacing is preferable for improving quantification of the NIR-TRS measurement to intracerebral hemodynamics. Additionally, 4 cm of optode spacing is a good setting to monitor cerebral hemodynamics response around the gray matter region. Contribution ratio of intracerebral tissue at 4 cm estimated about 70%, although it varies according to wavelength. NIR measurement is a simple and easy method to evaluate cerebral hemodynamics.

Acknowledgments

The authors would like to thank Mr. T. Hiruma for his constant support and encouragement. The authors are also grateful to Drs. Y. Tsuchiya and T. Yamashita for useful discussions.

Appendix A. Derive reduced scattering and absorption coefficients from temporal profiles

Behavior of photon within scattering and absorption media like a living body is expressed by the photon diffusion Eq. (1) (Patterson et al., 1989).

$$\frac{1}{v}\frac{\partial}{\partial t}\phi(r,t) - D\nabla^2\phi(r,t) + \mu_a\varphi(r,t) = S(r,t) \quad (1)$$

where $\phi(r, t)$ is the diffuse photon fluence rate at position r and time t, D is the photon diffusion coefficient and expressed in $D = 1/3\mu_s'$, v is the velocity of light within the media and $S(r, t)$ is the light source.

Solutions using this equation are found under different boundary conditions. We used the solution of a semi-infinite homogeneous model (Patterson et al., 1989) for TRS data analysis. In this solution, $R(d, t)$ is expressed by a function of the optode spacing, the reduced scattering coefficient (μ_s') and absorption coefficient (μ_a), as shown in Eq. (2).

$$R(d,t) = (4\pi Dv)^{-\frac{3}{2}} z_0 t^{-\frac{5}{2}} \exp(-\mu_a v t) \exp\left(-\frac{d^2 + z_0^2}{4Dvt}\right) \quad (2)$$

where d is the optode spacing and $z_0 = 1/\mu_s'$.

Using the non-linear least squares method, we fit Eq. (2) into the observed temporal profiles obtained from TRS and determined μ_s' and μ_a at each wavelength (Suzuki et al., 1994). The conversion chi-square (χ_v^2) value was adopted to evaluate fitting accuracy. We confirmed that our observed profiles fitted well with the theoretical curves using this index ($0.8 < \chi_v^2 < 1.2$; Grinvald and Steinberg, 1974).

Appendix B. Calculation of hemoglobin concentration and oxygen saturation by absorption coefficients

The μ_a of the 3 wavelengths (761, 791, 836 nm) that were measured is expressed as shown in simultaneous Eq. (3).

$$\begin{aligned}
\mu_{a761nm} &= \varepsilon_{oxyHb761nm} C_{oxyHb} + \varepsilon_{deoxyHb761nm} C_{deoxyHb} \\
&\quad + \varepsilon_{H_2O761nm} C_{H_2O} + \mu_{abkg761nm} \\
\mu_{a791nm} &= \varepsilon_{oxyHb791nm} C_{oxyHb} + \varepsilon_{deoxyHb791nm} C_{deoxyHb} \\
&\quad + \varepsilon_{H_2O791nm} C_{H_2O} + \mu_{abkg791nm} \\
\mu_{a836nm} &= \varepsilon_{oxyHb836nm} C_{oxyHb} + \varepsilon_{deoxyHb836nm} C_{deoxyHb} \\
&\quad + \varepsilon_{H_2O836nm} C_{H_2O} + \mu_{abkg836nm} \quad (3)
\end{aligned}$$

where μ_a is the absorption coefficient at the wavelength λ, $\varepsilon_{m\lambda}$ is the molar extinction coefficient of the substance m at the wavelength λ, C_m is the concentration of the substance m and bkg is the chromophores contributing to μ_a in tissue for other than oxygenated hemoglobin (oxyHb), deoxygenated hemoglobin (deoxyHb) and water.

Based on the assumption that light absorption in the living body in this wavelength region occurs from oxyHb, deoxyHb and water, and also that there is no other background absorption in the living body (Tromberg et al., 1997), we determined TRS values for oxygenated hemoglobin (TRS HbO_2) and deoxygenated hemoglobin (TRS Hb) as tissue water concentration is 70%.

TRS total hemoglobin (TRS tHb) and SO_2 were obtained from Eq. (4) as follows.

$$\text{TRS tHb}[\mu M] = \text{TRS } HbO_2 + \text{TRS Hb},$$

$$SO_2[\%] = \frac{\text{TRS } HbO_2}{\text{TRS tHb}} \times 100 \quad (4)$$

Appendix C. Conversion TRS tHb into TRS CBV

We converted the TRS tHb into the CBV by TRS (TRS CBV) using Eq. (5) (Wyatt et al., 1990) for comparison with the CBV by PET (PET CBV).

$$\text{TRS CBV}[\text{cc}/100\text{ g}] = \frac{\text{TRS tHb} \times MW_{Hb}}{Hb \times \eta \times \rho \times 100000} \quad (5)$$

where MW_{Hb} is hemoglobin molecular weight; 64,500, Hb is arterial hemoglobin concentration (g/dl) of subject, η is the cerebral-to-large-vessel hematocrit ratio; 0.85 (Phelps et al., 1979) and ρ is density of cerebral tissue (g/ml); 1.04 (Picozzi et al., 1985).

References

Bevilacqua, F., Piguet, D., Marquet, P., Gross, J.D., Tromberg, B.J., Depeursinge, C., 1999. In vivo local determination of tissue optical properties: applications to human brain. Appl. Opt. 38 (22), 4839–4950.

Brazy, J.E., Lewis, D.V., Mitnick, M.H., Jobsis, F.F., 1985. Noninvasive monitoring of cerebral oxygenation in preterm infants: preliminary observations. Pediatrics 75, 217–225.

Cope, M., Delpy, D.T., 1988. A system for long-term measurement of cerebral blood and tissue oxygenation in newborn infants by near infrared transillumination. Med. Biol. Eng. Comput. 26, 289–294.

De Blasi, R.A., Almenräder, N., Ferrari, M., 1997. Brain oxygenation monitoring during cardiopulmonary bypass by near infrared spectroscopy. Adv. Exp. Med. Biol. 413, 97–104.

Ehrenreich, D.L., Burns, R.A., Alman, R.W., Fazekas, J.F., 1961. Influence of acetazolamide on cerebral blood flow. Arch. Neurol. 5, 227–232.

Ferrari, M., Zanette, E., Sideri, G., Gianni, I., Fieschi, C., Carpi, A., 1987. Effects of carotid compression, as assessed by near infrared spectroscopy, upon cerebral volume and haemoglobin oxygen saturation. J. R. Soc. Med. 80, 83–87.

Firbank, M., Hiraoka, M., Essebpreis, M., Delpy, D.T., 1993. Measurement of the optical properties of the skull in the wavelength range 650–950 nm. Phys. Med. Biol. 38, 503–510.

Firbank, M., Schweiger, M., Delpy, D.T., 1995. Investigation of 'light piping' through clear regions of scattering objects. SPIE 2389, 167–173.

Germon, T.J., Evans, P., Barnett, N., Wall, P., Nelson, R.J., 1995. Optode separation determines sensitivity of near infrared spectroscopy to intra- and -external oxygenation changes. J. Cereb. Blood Flow Metab. 15, 617.

Grinvald, A., Steinberg, I.Z., 1974. On the analysis of fluorescence decay kinetics by the method of least-squares. Anal. Biochem. 59 (5), 583–598.

Harris, D.N.F., Cowans, F.M., Wertheim, D.A., Hamid, S., 1994. NIRS in adult-effects of increasing optode separation. Adv. Exp. Med. Biol. 345, 837–840.

Herscovitch, P., Markham, J., Raichle, M.E., 1983. Brain blood flow measured with intravenous H215O: I. Theory and error analysis. J. Nucl. Med. 24, 782–789.

Hillman, E., Hebden, J., Schweiger, M., Dehghani, H., Schmidt, F.E.W., Delpy, D.T., Arridge, S.R., 2001. Time resolved optical tomography of the human forearm. Phys. Med. Biol. 46, 1117–1130.

Isobe, K., Kusaka, T., Fujikawa, Y., Kondo, M., Yasuda, S., Itoh, S., Hirano, K., Onishi, S., 2000. Changes in cerebral hemoglobin concentration and oxygen saturation immediately after birth in the human neonate using full-spectrum near infrared spectroscopy. J. Biomed. Opt. 5 (3), 283–286.

Iwai, H., Urakami, T., Miwa, M., Nishizawa, M., Tsuchiya, Y., 2001. Tissue spectroscopy with a newly developed phase modulation system based on the microscopic Beer-Lambert law. SPIE 4250, 482–488.

Iwase, M., Ouchi, Y., Okada, H., Yokoyama, C., Nobezawa, S., Yoshikawa, E., Tsukada, H., Takeda, M., Yamashita, K., Takeda, M., Yamaguti, K., Kuratsune, H., Shimizu, A., Watanabe, Y., 2002. Neural substrates of human facial expression of pleasant emotion induced by comic films: a PET study. NeuroImage 17, 758–768.

Jobsis, F.F., 1977. Noninvasive, infrared monitoring of cerebral and myocardial oxygen sufficiency and circulatory parameters. Science 198, 1264–1267.

Kakihana, Y., Matsunaga, A., Yamada, H., Dohgomori, H., Oda, T., Yoshimura, N., 1996. Continuous, noninvasive measurement of cytochrome oxidase in cerebral cortex by near-infrared spectrophotometry during aortic arch surgery. J. Anesth. 10, 221–224.

Kohri, S., Hoshi, Y., Tamura, M., Kato, C., Kuge, Y., Tamaki, N., 2001. Quantitative evaluation of the relative contribution ratio of cerebral tissue to near-infrared signals in adult human head. A preliminary study. Physiol. Meas. 23 (2), 301–312.

Lammertsma, A.A., Jones, T., 1983. Correction for the presence of intravascular oxygen-15 in the steady-state technique for measuring regional oxygen extraction ratio in the brain: 1. Description of the method. J. Cereb. Blood Flow Metab. 3, 416–424.

Lammertsma, A.A., Baron, J.C., Jones, T., 1987. Correction for intravascular activity in the oxygen-15 steady-state technique is independent of the regional hematocrit. J. Cereb. Blood Flow Metab. 7, 372–374.

McCormick, P.W., Stewart, M., Lewis, G., Dujovny, M., Ausman, J.I., 1992. Intracerebral penetration of infrared light. J. Neurosurg. 76 (2), 315–319.

Meek, J.H., Elwell, C.E., McCormick, D.C., Edwards, A.D., Townsend, J.P., Stewart, A.L., Wyatt, J.S., 1999. Abnormal cerebral haemodynamics in perinatally asphyxiated neonates related to outcome. Arch. Dis. Child., Fetal Neonatal Ed. 81 (2), F110–F115 (Sep).

Misonoo, S., Okada, E., 2001. Adult head modeling based on time-resolved measurement for NIR instrument. SPIE 4250, 522–529.

Oda, M., Yamashita, Y., Nishimura, G., Tamura, M., 1996. A simple and novel algorithm for time-resolved multiwavelength oximetry. Phys. Med. Biol. 41, 551–562.

Oda, M., Nakano, T., Suzuki, A., Shimizu, K., Hirano, I., Shimomura, F., Ohmae, E., Suzuki, T., Yamashita, Y., 2000. Nearinfrared time-resolved spectroscopy system for tissue oxygenation monitor. SPIE 4160, 204–210.

Okada, E., Delpy, D.T., 2000. Effects of scattering of arachnoid trabeculae on light propagation in the adult brain. Advances in optical imaging, photon migration, and tissue optics. OSA Tech. Dig. 256–258.

Okada, E., Delpy, D.T., 2003a. Near-infrared light propagation in an adult head model: I. Modeling of low-level scattering in the cerebrospinal fluid layer. Appl. Opt. 42 (16), 2906–2914.

Okada, E., Delpy, D.T., 2003b. Near-infrared light propagation in an adult head model: II. Effect of superficial tissue thickness on the sensitivity of the near-infrared spectroscopy signal. Appl. Opt. 42 (16), 2915–2922.

Okada, E., Firbank, M., Schweiger, M., Arridge, S.R., Cope, M., Delpy, D.T., 1997. Theoretical and experimental investigation of near-infrared light propagation in a model of the adult head. Appl. Opt. 36 (1), 21–31.

Ouchi, Y., Nobezawa, S., Okada, H., Yoshikawa, E., Futatsubashi, M., Kaneko, M., 1998. Altered glucose metabolism in the hippocampal head in memory impairment. Neurology 51, 136–142.

Ouchi, Y., Okada, H., Yoshikawa, E., Futatsubashi, M., Nobezawa, S., 2001. Absolute changes in regional cerebral blood flow in association with upright posture in humans: an orthostatic PET study. J. Nucl. Med. 42, 707–712.

Patterson, M.S., Chance, B., Wilson, B.C., 1989. Time resolved reflectance and transmittance for the noninvasive measurement of tissue optical properties. Appl. Opt. 28 (12), 2331–2336.

Phelps, M.E., Huang, S.C., Hoffman, E.J., Kuhl, D.E., 1979. Validation of tomographic measurement of cerebral blood volume with C-11-labeled carboxyhemoglobin. J. Nucl. Med. 20, 328–334.

Picozzi, P., Todd, N.V., Crockard, A.H., 1985. The role of cerebral blood volume changes in brain specific-gravity measurements. J. Neurosurg. 62 (5), 704–710 (May).

Posner, J.P., Plum, F., 1960. The toxic effects of carbon dioxide and acetazolamide in hepatic encephalopathy. J. Clin. Invest. 39, 1246–1258.

Suzuki, K., Yamashita, Y., Ohta, K., Chance, B., 1994. Quantitative measurement of optical parameters in the breast using time-resolved spectroscopy. Invest. Radiol. 29 (4), 410–414.

Suzuki, S., Takasaki, S., Ozaki, T., Kobayashi, Y., 1999. A tissue oxygenation monitor using NIR spatially resolves spectroscopy. SPIE 3597, 582–592.

Tanosaki, M., Hoshi, Y., Iguchi, Y., Oikawa, Y., Oda, I., Oda, M., 2001. Variation of temporal characteristics in human cerebral hemodynamic responses to electric median nerve stimulation: a near-infrared spectroscopic study. Neurosci. Lett. 316, 75–78.

Torricelli, A., Pifferi, A., Taroni, P., Giambattistelli, E., Cubeddu, R., 2001. In vivo optical characterization of human tissues from 610 to 1010 nm by time-resolved reflectance spectroscopy. Phys. Med. Biol. 46, 2227–2237.

Tromberg, B.J., Coquoz, O., Fishkin, J.B., Pham, T., Anderson, E., Butler, J., Cahn, M., Gross, J.D., Venugopalan, V., Pham, D., 1997. Non-invasive measurements of breast tissue optical properties using frequency-domain photon migration. Philos. Trans. R. Soc. Lond., B 352, 661–668.

Tuchiya, Y., Urakami, T., 1996. Frequency domain analysis of photon migration based on the microscopic Beer-Lambert law. Jpn. J. Appl. Phys. 35, 4848–4851.

Ueda, U., Ohta, K., Oda, M., Miwa, M., Tsuchiya, Y., Yamashita, Y., 2001. 3-D imaging of a tissue-like phantom by diffusion optical tomography. Appl. Opt. 40 (34), 6349–6355.

Van der Zee, P., Cope, M., Arridge, S.R., Essenpreis, M., Potter, L.A., Edwards, A.D., Wyatt, J.S., McCormick, D.C., Roth, S.C., Reynolds, E.O.R., Delpy, D.T., 1992. Experimentally measured optical pathlength for the adult head, calf and forearm and the head of the newborn infant as a function of inter optode spacing. Exp. Med. Biol. 316, 143–153.

Vorstrup, S., Henriksen, L., Paulson, O., 1984. Effect of acetazolamide on cerebral blood flow and cerebral metabolic rate for oxygen. J. Clic. Invest. 74, 1634–1639.

Watanabe, E., Maki, A., Kawaguchi, F., Yamashita, Y., Koizumi, H., Mayanagi, Y., 2000. Noninvasive cerebral blood volume measurement during seizures using multichannel near infrared spectroscopic topography. J. Biomed. Opt. 5 (3), 287–290.

Wyatt, J.S., Cope, M., Delpy, D.T., Richardson, C.E., Edwards, A.D., Wray, S., Reynolds, E.O.R., 1990. Quantitation of cerebral blood volume in human infants by near-infrared spectroscopy. J. Appl. Physiol. 68, 1086–1091.

Yamashita, Y., Oda, M., Ohmae, E., Tamura, M., 1998. Continuous measurement of oxy- and deoxyhemoglobin of piglet brain by time-resolved spectroscopy. OSA TOPS 22, 205–207.

Zhang, H., Miwa, M., Urakami, T., Yamashita, Y., Tsuchiya, Y., 1998. Simple subtraction method for determining the mean path length traveled by photons in turbid media. Jpn. J. Appl. Phys. 37, 700–704.

Available online at www.sciencedirect.com
ScienceDirect
Neuroscience Letters 407 (2006) 131–135
Neuroscience Letters
www.elsevier.com/locate/neulet

Changes in cerebral blood flow under the prone condition with and without massage

Yasuomi Ouchi [a,*], Toshihiko Kanno [a], Hiroyuki Okada [b], Etsuji Yoshikawa [b], Tomomi Shinke [b], Shingo Nagasawa [c], Keiji Minoda [d], Hiroyuki Doi [e]

[a] *Positron Medical Center, Hamamatsu Medical Center, 5000 Hirakuchi, Hamamatsu 434-0041, Japan*
[b] *Central Research Laboratory, Hamamatsu Photonics K.K., Hamamatsu, Japan*
[c] *Yanaihara Laboratory, Fuji, Japan*
[d] *Balance Therapy University, Fukuoka, Japan*
[e] *Shizuoka Prefectural Government, Shizuoka, Japan*

Received 17 May 2006; received in revised form 25 July 2006; accepted 10 August 2006

Abstract

To investigate changes in regional cerebral blood flow (rCBF) under the prone condition with and without light massage on the back, we measured rCBF quantitatively in healthy human subjects using positron emission tomography with $H_2{}^{15}O$. Biochemical tests showed that the light massage (palm-pressure) reduced levels of stress-related serum cortisol and salivary stress protein chromogranin-A measured after the PET examination. Absolute rCBF significantly increased in the parietal cortex (precuneus) under the prone condition compared with the supine condition, and this rCBF increase was in parallel with comfortable sensation and slowing heart rate during the massage. Correlation analysis in statistical parametric mapping showed that the amygdalar and basal forebrain rCBF correlated with parasympathetic function (heart rate reduction), indicating involvement of the forebrain-amygdala system in mediating activities in the autonomic nervous system in the presence of comfortable sensation. To conclude, prone posture itself can stimulate the precuneus region to raise awareness, and the light massage on the back may help accommodate the brain to comfortable stimulation.

Keywords: Prone posture; Palm-pressure massage; Cerebral blood flow; Positron emission tomography; Precuneus

A prone posture is what people sometimes assume for a quick rest in the daily living and is a common style during massage therapy. It is well accepted that massage therapy gives positive effects on physical and mental care irrespective of health conditions [4,18,23]. Specifically, moderate pressure massage is reported to cause reductions in heart rate and in alpha and beta activities on electroencephalography (EEG), indicating generation of a relaxation response [23]. Biochemical basic studies also indicated massage-related favorable changes in the immune [8] and neurohormonal systems [22]. Thus, we hypothesized that the maneuver could alter brain activity in a specific region that relates to autonomic nervous system.

Exploration of brain activation can be achieved by using neuroimaging techniques such as positron emission tomography (PET) and functional magnetic resonance imaging (fMRI) in the field of complementary alternative medicine, e.g. acupuncture [2,13]. We have recently developed a new imaging method that enables to scan human subjects on the prone condition using PET [16]. This technique allows us to investigate the effect of back massage on regional cerebral blood flow (rCBF) quantitatively. Previous studies indicate that the inferomedial region of the frontal cortex and amygdala are likely to play central roles in relaxation processing [11,14] and that the precuneus engages in the integration of multiple neural systems producing a conscious self-percept [1]. Thus, the purpose of the present study was to examine absolute changes in rCBF in the prone posture with and without massage applied on the back using PET with $H_2{}^{15}O$.

Eight right-handed healthy volunteers (4 male, 4 female; mean age ± S.D., 40.2 ± 10.7 years) participated in the current study. All participants had neither neurological problems nor habits of regular intake of over-the-counter pills, and were naïve

* Corresponding author. Tel.: +81 53 585 0366; fax: +81 53 585 0367.
E-mail address: ouchi@pmc.hmedc.or.jp (Y. Ouchi).

0304-3940/$ – see front matter © 2006 Published by Elsevier Ireland Ltd.
doi:10.1016/j.neulet.2006.08.037

to the current palm-pressure massage. The present study was approved by the Ethics Committee of the Hamamatsu Medical Center, and written informed consent was obtained from all participants. To examine stress neuroendocrinologically, we measured salivary levels of chromogranin-A, a protein induced by mental stress [10,15] and cortisol in blood [20] before and after the measurement.

Three-dimensional MRI by a 0.3 T scanner (MRP7000AD, Hitachi, Tokyo, Japan) revealed no morphological abnormalities. Then, a maximum of four to six PET scans were performed under the following conditions with all eyes closed; (a) supine at rest, (b) prone at rest, (c) prone with back massage at an early stage (4 min after the stimulation, Stim-1), (d) prone with back massage at a later stage (20 min after the stimulation, Stim-2). The massage was performed in a similar manner over the back target region. Two professional therapists from Balance Therapy University performed palm-pressure massage onto the back muscles including trapezius, rhombodeus and latissimus dorsi for nearly 24 min, consecutively.

Using a brain-purpose PET scanner (SHR12000, Hamamatsu Photonics, Hamamatsu, Japan), we performed quantitative measurement of rCBF in a conventional way [7,17] but in a different condition in which arterial blood was sampled continuously through the catheter inserted in the left brachial artery while the examinee was lying on his/her stomach during the PET scan. The dose of $H_2{}^{15}O$ injected was set 300 MBq/scan for each measurement. To establish the reproducible measurement under the prone posture, we used a thermoplastic facemask attached firmly to the scanner's couch during the prone condition, which allowed the volunteer to be secured in the gantry and to avoid misregistration artifacts [16]. The heart rate, arterial blood pressure and skin temperature were monitored simultaneously during scans. The subjective visual analog scale (VAS) for relaxation (ranging from 1 to 10, 1 being the most uncomfortable to 10 being the most comfortable) was rated after each PET scan.

Each rCBF value was calculated based on a region of interest (ROI) method, in which semicircular ROIs were placed over the cerebellum, lower frontal area (Brodmann area or BA: 10/11), upper frontal area (BA: 6/8), temporal (BA: 21/22), parietal (BA: 7), occipital (BA: 17/18) cortices, the striatum and the thalamus on the MR images and the corresponding PET images [16]. Repeated measures analysis of variance (ANOVA) was used for analyzing changes in rCBF among the present conditions. Following a Bonferroni post hoc test, a p-value less than 0.05 was regarded as statistically significant. In addition, we performed a voxel-wise mapping analysis using SPM2 (Wellcome Department of Cognitive Neurology, University College, London) to elucidate brain loci significantly activated during the massage. Voxel-based correlations were computed between physiological parameters and rCBF using VAS scores as confounding covariates, and the statistical threshold was set at $p = 0.001$ uncorrected for peak height and at clusters over 50 contiguous voxels.

Among physiological parameters, a significant reduction was observed only in heart rate during the Stim-2 condition (Table 1, Fig. 1D). The χ^2-test disclosed that the concentrations of salivary chromogranin-A and plasma cortisol were significantly lower after PET examination (0.8 ± 1.0 pmol/mg-protein

Table 1
Results of physiology and cerebral blood flow during each condition

Condition	Physiology			Cerebral blood flow (ml/100g/min)							
	MABP (mmHg)	Heart rate (b/m)	Temperature (°C)	Cerebellum	Lower frontal	Upper frontal	Temporal	Parietal	Occipital	Thalamus	Striatum
Supine	81.1 ± 8.3	71.2 ± 9.8	N.E.	51.1 ± 7.3	45.4 ± 5.9	50.0 ± 6.2	49.9 ± 4.9	49.3 ± 6.4	46.5 ± 7.2	54.5 ± 6.8	56.8 ± 8.3
Prone	81.7 ± 11.7	70.6 ± 11.1	33.66 ± 0.37	58.4 ± 9.3	48.0 ± 7.9	53.6 ± 9.4	50.5 ± 7.3	51.2 ± 7.7	50.9 ± 8.3	61.8 ± 9.0	58.1 ± 9.7
Stim-1	80.4 ± 7.3	69.7 ± 9.9	33.61 ± 0.19	60.8 ± 10.1	47.3 ± 5.8	52.6 ± 9.2	53.3 ± 7.5	54.4 ± 7.7	52.2 ± 7.3	60.3 ± 9.2	58.6 ± 8.7
Stim-2	81.7 ± 11.4	66.9† ± 10.3	33.74 ± 0.28	60.3 ± 9.7	47.9 ± 7.1	54.7 ± 9.5	54.6 ± 8.3	57.6 ± 8.9*†	57.0 ± 9.4*	62.0 ± 7.8	60.6 ± 8.8

Values are expressed as mean ± S.D. MABP: mean arterial blood pressure. *$p < 0.05$ vs. supine condition, †$p < 0.05$ vs. prone condition.

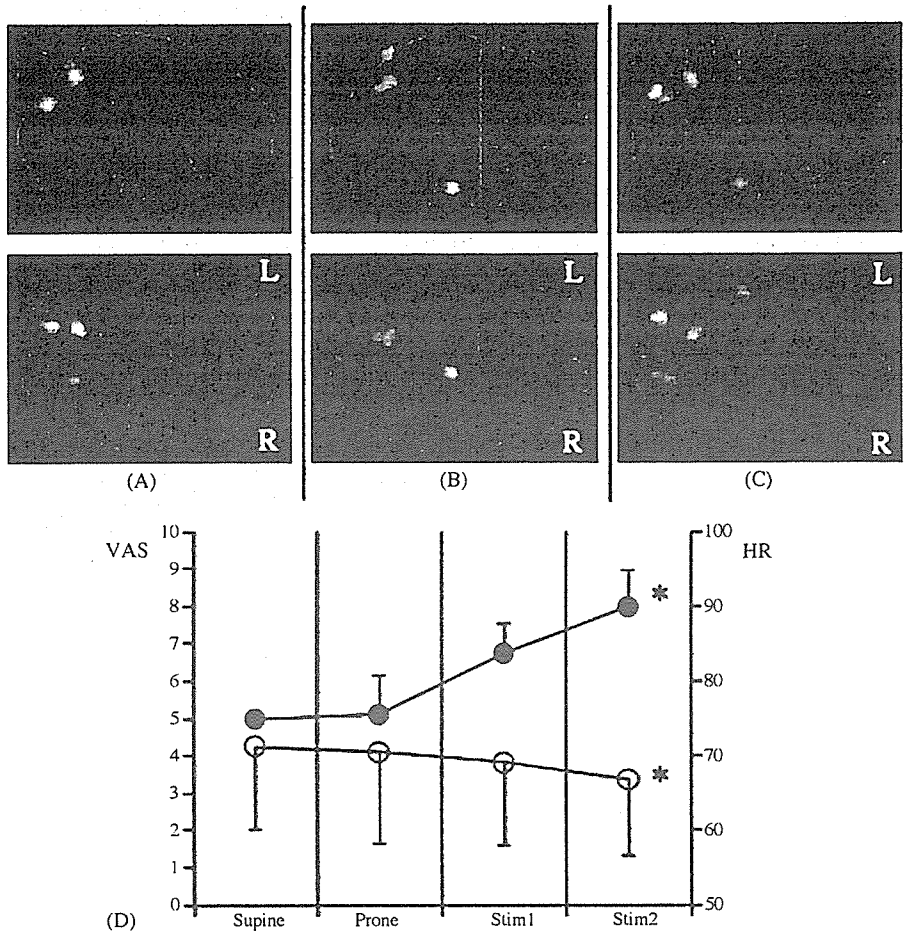

Fig. 1. Brain regions significantly activated during the prone condition vs. the supine condition (A), during the Stim-1 vs. the prone condition (B), and during the Stim-2 vs. the prone condition (C). (D) Changes in visual analog scale (VAS, ●) for relaxation and heart rate (HR, ○).

and 5.4 ± 3.4 μg/dl, respectively) than before (1.2 ± 1.7 and 6.4 ± 3.8 μg/dl, respectively), suggesting reduction in mental stress. This speculation was consistent with the finding that the VAS score for positive affect was much higher after the Stim-2 condition (Fig. 1D).

Repeated measures ANOVA showed significant increase in absolute rCBF in the parietal and occipital cortices during the Stim-2 condition compared with rCBF in the supine condition (Table 1). The parietal rCBF was also significantly higher in the Stim-2 condition than that in the prone condition. There was a tendency of rCBF elevation after assuming of prone posture in comparison with the supine posture in general.

Examination of relative increase in rCBF in the brain using voxel-based subtraction analysis in SPM2 revealed a significant elevation in rCBF in the precuneus bilaterally during the prone condition versus the supine condition (Talairach coordinates: $xyz = -18\ -62\ 50$, $Z = 5.1$; $16\ -64\ 58$, $Z = 4.6$) (Fig. 1A). Comparison of the Stim-1 condition with the prone condition showed significant increase in rCBF in the left precuneus and pons ($8\ -18\ -28$, $Z = 4.6$) (Fig. 1B). Compared with the prone condition, significant rCBF increase was found in the bilateral precuneus and left fusiform gyrus ($xyz = -46\ -28\ -24$, $Z = 4.7$) during the Stim-2 condition (Fig. 1C), in which the VAS and heart rate were significantly elevated (Fig. 1D). Correlation analysis showed a significant positive correlation of heart rate reduction with rCBF in the bilateral amygdala, orbitofrontal, hypothalamus (infundibulum) and cerebellar vermis (Fig. 2).

The present study was the first to measure rCBF quantitatively in the prone posture under palm-pressure massage applied to the back. Because each participant was released from a restraint of prone posture and allowed to sit just after each PET scan, there was less chance of a protracted prone-posture effect itself. We found that prolonged palm-pressure stimulation activated the precuneus and fusiform, along with a greater increase in parasympathetic activity and comfortable valence under the conscious state of mind. Thus, the present therapeutic maneuver may operate on the parieto-occipital region and stimulate the parasympathetic system. The present activation was in accordance with a previous report that the medial occipital cortex and lower parietal cortex were activated by relief-inducing electroacupuncture possibly through somatic-visceral sensory stimulation [24]. In addition, no increase in absolute rCBF in the frontal cortex during the present back stimulation was in line with the result from a previous PET study on hypnotics showing that the hypnotic condition caused rCBF reduction in the frontal lobe [9]. Thus, generation of comfortable sensation by the back massage may be related to rCBF increase in the posterior brain region, specifically the precuneus.

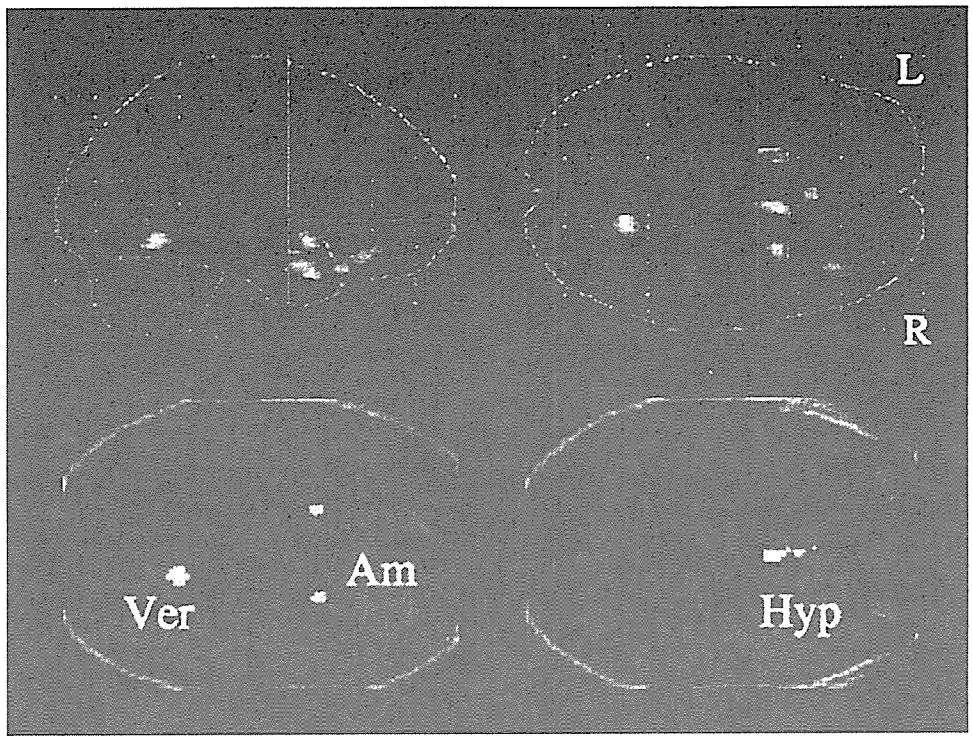

Fig. 2. Brain regions significantly correlated with reduction in heart rate. Am, amygdala; Ver, cerebellar vermis; Hyp, hypothalamus (infundibulum).

The reason for rCBF increase in the posterior brain region remains yet to be explored, but there are pieces of evidence to be noted. Regional CBF in the occipital lobe increases in a state of reduction in vigilance in parallel with the slow wave activity on electroencephalogram [19]. Visually-induced grief generates an activation of the inferior temporal and fusiform gyri [5]. The precuneus is involved in the integration of the neural network for self-consciousness, engaged in self-related mental representation [1]. In contrast, deactivation of the precuneus may indicate a loss of higher-order body or self-representation [12]. Thus, the precuneus is considered again, to play an important role in the internal mentation processes of awareness [1]. In other word, the activation of the precuneus by the back massage may reflect an augmentation of arousal and consciousness functions for positive affect.

The present VAS and neurohormonal findings verified the efficacy of the present back stimulation to reduce mental stress or anxiety in an objective sense. Before interpreting the current back massage effect, though, the methodological limitations have to be recognized because we did not apply any different types of massage that would induce mental relaxation and because we did not perform polysomnography to rule out a contamination form an early stage of sleep. However, the previous report about this massage and prompt volitional reactions just after each PET measurement (no one fell into sleep) would support the occurrence of palm-pressure effect on the neuronal and cognitive basis. In the voxel-wise correlation analysis, the bilateral amygdala, basal forebrain and cerebellar vermis were associated with reduction in heart rate. Because a PET study on biofeedback relaxation effect indicated that the region close to the hypothalamus-amygdala system serves in reducing the sympathetic bodily responses to stress and anxiety [3], the current back stimulation might affect this forebrain-amygdala system into augmenting the parasympathetic tone in the brain. The significant correlation in the cerebellum likely implies cerebellar contribution to regulating the parasympathetic system because the cerebellum is reciprocally connected to the hypothalamus, enabling to engage in the neural circuit governing autonomic function [21].

In conclusion, a prone-posture itself raises absolute rCBF in the awareness-related posterior brain region, and this rCBF increase was in association with relaxed feeling induced by back massage. The present result provided scientific evidence on its efficacy of palm-pressure massage to generate mental relaxation possibly by modulating neuronal activities in the forebrain-amygdala and precuneus network because happiness affect might be associated with the activation of the amygdala and posterior part of the cingulate cortex such as the precuneus [6].

Acknowledgments

The authors would like to thank Mr. Kenji Suzuki, Mrs. Dari Terashima, Hitomi Kimura (Balance Therapy University), Mr. Yutaka Naito (Nippon Environment Research KK), and the staff of the Positron Medical Center (Hamamatsu Medical Center) for their technical support. This study was supported by research grant from the Ministry of Health, Labor, and Welfare, Tokyo.

References

[1] A.E. Cavanna, M.R. Trimble, The precuneus: a review of its functional anatomy and behavioural correlates, Brain 129 (2006) 564–583.

[2] Z.H. Cho, S.C. Chung, J.P. Jones, J.B. Park, H.J. Park, H.J. Lee, E.K. Wong, B.I. Min, New findings of the correlation between acupoints and corresponding brain cortices using functional MRI, Proc. Natl. Acad. Sci. U.S.A. 95 (1998) 2670–2673.
[3] H.D. Critchley, R.N. Melmed, E. Featherstone, C.J. Mathias, R.J. Dolan, Brain activity during biofeedback relaxation: a functional neuroimaging investigation, Brain 124 (2001) 1003–1012.
[4] M.A. Diego, T. Field, C. Sanders, M. Hernandez-Reif, Massage therapy of moderate and light pressure and vibrator effects on EEG and heart rate, Int. J. Neurosci. 114 (2004) 31–44.
[5] H. Gundel, M.F. O'Connor, L. Littrell, C. Fort, R.D. Lane, Functional neuroanatomy of grief: an FMRI study, Am. J. Psychiatry 160 (2003) 1946–1953.
[6] U. Habel, M. Klein, T. Kellermann, N.J. Shah, F. Schneider, Same or different? Neural correlates of happy and sad mood in healthy males, Neuroimage 26 (2005) 206–214.
[7] P. Herscovitch, J. Markham, M.E. Raichle, Brain blood flow measured with intravenous H215O. I. Theory and error analysis, J. Nucl. Med. 24 (1983) 782–789.
[8] G. Ironson, T. Field, F. Scafidi, M. Hashimoto, M. Kumar, A. Kumar, A. Price, A. Goncalves, I. Burman, C. Tetenman, R. Patarca, M.A. Fletcher, Massage therapy is associated with enhancement of the immune system's cytotoxic capacity, Int. J. Neurosci. 84 (1996) 205–217.
[9] N. Kajimura, M. Nishikawa, M. Uchiyama, M. Kato, T. Watanabe, T. Nakajima, T. Hori, T. Nakabayashi, M. Sekimoto, K. Ogawa, H. Takano, E. Imabayashi, M. Hiroki, T. Onishi, T. Uema, Y. Takayama, H. Matsuda, M. Okawa, K. Takahashi, Deactivation by benzodiazepine of the basal forebrain and amygdala in normal humans during sleep: a placebo-controlled [^{15}O]H_2O PET study, Am. J. Psychiatry 161 (2004) 748–751.
[10] T. Kanno, N. Asada, H. Yanase, T. Iwanaga, T. Ozaki, Y. Nishikawa, K. Iguchi, T. Mochizuki, M. Hoshino, N. Yanaihara, Salivary secretion of highly concentrated chromogranin a in response to noradrenaline and acetylcholine in isolated and perfused rat submandibular glands, Exp. Physiol. 84 (1999) 1073–1083.
[11] S.W. Lazar, G. Bush, R.L. Gollub, G.L. Fricchione, G. Khalsa, H. Benson, Functional brain mapping of the relaxation response and meditation, Neuroreport 11 (2000) 1581–1585.
[12] P. Maquet, M.E. Faymonville, C. Degueldre, G. Delfiore, G. Franck, A. Luxen, M. Lamy, Functional neuroanatomy of hypnotic state, Biol. Psychiatry 45 (1999) 327–333.
[13] V. Napadow, N. Makris, J. Liu, N.W. Kettner, K.K. Kwong, K.K. Hui, Effects of electroacupuncture versus manual acupuncture on the human brain as measured by fMRI, Hum. Brain Mapp. 24 (2005) 193–205.
[14] A. Newberg, A. Alavi, M. Baime, M. Pourdehnad, J. Santanna, E. d'Aquili, The measurement of regional cerebral blood flow during the complex cognitive task of meditation: a preliminary SPECT study, Psychiatry Res. 106 (2001) 113–122.
[15] V. Ng, D. Koh, B.Y. Mok, S.E. Chia, L.P. Lim, Salivary biomarkers associated with academic assessment stress among dental undergraduates, J. Dent. Educ. 67 (2003) 1091–1094.
[16] Y. Ouchi, T. Kanno, E. Yoshikawa, T. Ogusu, H. Okada, K. Minoda, H. Doi, Neural correlates of muscle relaxation stimulation in the human brain, Neurosci. Res. 52 (2005) S119.
[17] Y. Ouchi, H. Okada, E. Yoshikawa, M. Futatsubashi, S. Nobezawa, Absolute changes in regional cerebral blood flow in association with upright posture in humans: an orthostatic PET study, J. Nucl. Med. 42 (2001) 707–712.
[18] O.Y. Oumeish, The cultural and philosophical aspects of pressure, massage, and touch healing as alternative therapies, Skinmed 4 (2005) 93–100.
[19] T. Paus, R.J. Zatorre, N. Hofle, Z. Caramanos, J. Gotman, M. Petrides, A.C. Evans, Time-related changes in neural systems underlyiing attention and arousal during the performance of an audiroty vigilance task, J. Cogn. Neurosci. 9 (1997) 392–408.
[20] M.D. Sauro, R.S. Jorgensen, C.T. Pedlow, Stress, glucocorticoids, and memory: a meta-analytic review, Stress 6 (2003) 235–245.
[21] J.D. Schmahmann, D. Caplan, Cognition, emotion and the cerebellum, Brain 129 (2006) 290–292.
[22] S. Wikstrom, T. Gunnarsson, C. Nordin, Tactile stimulus and neurohormonal response: a pilot study, Int. J. Neurosci. 113 (2003) 787–793.
[23] D.L. Woods, M. Dimond, The effect of therapeutic touch on agitated behavior and cortisol in persons with Alzheimer's disease, Biol. Res. Nurs. 4 (2002) 104–114.
[24] M.T. Wu, J.M. Sheen, K.H. Chuang, P. Yang, S.L. Chin, C.Y. Tsai, C.J. Chen, J.R. Liao, P.H. Lai, K.A. Chu, H.B. Pan, C.F. Yang, Neuronal specificity of acupuncture response: a fMRI study with electroacupuncture, Neuroimage 16 (2002) 1028–1037.